Journal of Hydrology 617 (2023) 129134

Contents lists available at ScienceDirect

Journal of Hydrology

journal homepage: www.elsevier.com/locate/jhydrol

Research papers

Dominant source areas shift seasonally from longitudinal to lateral contributions in a montane headwater stream

Sidney A. Bush [a,b,*], Andrew L. Birch [c], Sara R. Warix [d], Pamela L. Sullivan [e], Michael N. Gooseff [a,f], Diane M. McKnight [a,f], Holly R. Barnard [a,b]

[a] Institute of Arctic and Alpine Research, University of Colorado Boulder, Boulder, CO, USA
[b] Geography Department, University of Colorado Boulder, Boulder, CO, USA
[c] Water Resources Division, National Park Service, Fort Collins, CO, USA
[d] Hydrologic Science and Engineering, Colorado School of Mines, Golden, CO, USA
[e] College of Earth, Ocean, and Atmospheric Science, Oregon State University, Corvallis, OR, USA
[f] Civil, Environmental, and Architectural Engineering Department, University of Colorado Boulder, Boulder, CO, USA

ARTICLE INFO

Keywords:
Hydrologic connectivity
End-member mixing
Semi-arid
Chemical tracers
Non-perennial

ABSTRACT

Montane ecoregions are important vehicles for downstream hydrologic function, but their dynamics are relatively understudied compared to alpine and subalpine catchments in the western United States. Montane catchments experience shifts in precipitation inputs seasonally, which results in spatiotemporal differences in source area contributions to the stream. We collected hydrometric and geochemical data between 2018 and 2021 from a 2.65 km^2 semi-arid headwater catchment in the Front Range of Colorado, USA. Using a combined approach of hydrometric monitoring, geochemical characterization, and end-member mixing analysis (EMMA), we assess hydrologic connectivity between areas with high upslope accumulation and the stream. Within our study area, high upslope accumulation area corresponded to alluvial/ colluvial fans wherein we focused instrumentation and water sample collection. Using observed rainfall, and multiyear measurements of groundwater levels, soil moisture, and streamflow, we observed distinct hydrologic seasons within our catchment characterized by snowmelt during the spring, rainstorms during the summer, and a return to baseflow during the fall. Within this framework, we found that source areas to streamflow shift with longitudinal distance downstream, and among hydrologic seasons. Notably, our EMMA results indicate that contributions from upstream source areas become less important than lateral inputs from spring snowmelt into the fall return to baseflow. This was most pronounced at the upper catchment where upstream contributions to streamflow decreased up to 33.3% between spring and fall. These results suggest that streamflow is maintained by local source areas contributing laterally and vertically. Our results reflect dynamic shifts in hydrologic connectivity in space and in time, which are increasingly important to land and water resource management given rapid climate changes within the western United States.

1. Introduction

Within United States (US) western montane regions, headwater and non-perennial streams play an important role in the delivery of water, sediment, and nutrients downstream, and are vital to maintaining ecosystem health (Acuña et al., 2014; Buttle et al., 2012; Stubbington et al., 2017). Despite their importance, catchments in these regions are relatively understudied compared to higher elevation alpine catchments with persistent snowpack because they contribute less downstream discharge per unit drainage area than high alpine regions (Hammond et al., 2018; Jacobs, 2011; Viviroli et al., 2007). However, lower elevation catchments cover a large area, making our understanding of their cumulative contributions to downstream discharge important for water resource management (Harrison et al., 2021). In particular, in the western US, lower elevation, montane areas with intermittent snow persistence cover 25% of the land surface, compared to alpine regions with high snow persistence (> 50% of time with snow on the ground between Jan 1 and Jul 3) which only constitute 13% of the land surface (Moore et al., 2015). Future climate projections of warming temperatures suggest that areas with high snow persistence will decline

* Corresponding author at: 4001 Discovery Drive, Boulder, CO 80303, USA.
E-mail address: sidney.bush@colorado.edu (S.A. Bush).

https://doi.org/10.1016/j.jhydrol.2023.129134

Available online 16 January 2023

substantially in the coming decades with precipitation inputs shifting towards summer rain-events rather than snowmelt (Klos et al., 2014). Headwater and non-perennial stream systems are particularly sensitive to these climatic shifts, as changes in precipitation inputs cause a decline in connectivity between the terrestrial landscape of a catchment and the stream channel, decreasing streamflow permanence (Eng et al., 2016; Ward et al., 2020). Improving our understanding of spatial and temporal shifts in hydrologic connectivity in montane systems will become increasingly important both within the context of climate change in intermittent snow regions, and in better predicting how catchment function in regions with high snow persistence may change in the future. In many parts of the western US, shifts from snowmelt to rainfall dominated flow regimes have already been observed (Fritze et al., 2011; Kampf & Lefsky, 2016). A shift from snowmelt to rainfall inputs causes a change in water availability and temperature (Hunsaker et al., 2012), vegetation and plant water use (Hu et al., 2010), and subsurface water storage in soils and bedrock (Liu et al., 2013; Smith et al., 2011). Such changes can alter the paths by which water flows through a landscape (hydrologic flow paths) and is ultimately delivered to a stream (hydrologic connectivity) (Hinckley et al., 2014). For example, within alpine regions with high snow persistence, hydrologic connectivity between the catchment and the stream is generated largely through the hydrologic flow paths of saturation overland flow and subsurface flow (Cowie et al., 2017; Kampf et al., 2015; Liu et al., 2004). In montane regions with less snow accumulation and a shorter duration of snow cover, saturation overland flow from the catchment to the stream is rare, and lateral subsurface flow between the catchment and the stream may develop instead (Liu et al., 2013; McNamara et al., 2005). However, the spatiotemporal extent of hydrologic connectivity between the landscape and the stream through lateral subsurface flow is variable and depends on soil characteristics and precipitation inputs (Burns et al., 2001; Hinckley et al., 2014).

Hydrologic connectivity is inherently dynamic in that connections or disconnections can occur seasonally (Godsey & Kirchner, 2014; Whiting & Godsey, 2016) or episodically during rainfall or snowmelt pulses (Bracken & Croke, 2007; Jencso & McGlynn, 2011; Stieglitz et al., 2003; van Meerveld et al., 2015). Hydrologic connectivity of a landscape to the stream can expand and contract as runoff source areas shift through space and time, making it difficult to quantify. Consequently, hydrologic connectivity is often inferred from either stream-based or upland-based measurements because direct observations are limited due to the difficulty in observing and quantifying surface and subsurface processes (Blume & van Meerveld, 2015; Hopp & McDonnell, 2009). Studies commonly use natural or applied tracers through end-member mixing analysis (EMMA) to identify sources of water contributing to streamflow (Birch et al., 2021; Christophersen & Hooper, 1992; Hooper et al., 1990; Hooper & Shoemaker, 1986; Kiewiet et al., 2020; Sklash and Farvolden, 1979) and to assess connectivity of uplands to the stream (Tetzlaff et al., 2015; Uhlenbrook et al., 2004). Because stream chemistry is the proportional mixture of all actively contributing source areas within a catchment, chemically quantifying each source area, or end-member, allows for quantification of hydrologic connectivity between source areas within the catchment to the stream.

Source areas that contribute to streamflow are controlled by heterogeneity in both the surface features (e.g., topography, vegetation) and subsurface features (e.g., regolith depth, soil structure), and warrant both hydrometric and geochemical characterization to determine hydrologic connectivity (e.g., Burns et al., 2001). Previous studies have measured upland-stream connectivity using hydrometric measurements of the subsurface including topography, soil moisture, and quantification of the active drainage network (D'Odorico and Rigon, 2003; Jencso et al., 2009; Nippgen et al., 2015; Smith et al., 2013). Jencso et al. (2009) closely monitored water table levels installed along the hillslope to riparian slopes within the Tenderfoot Creek Experimental Forest in the northern Rocky Mountains of Montana and found that lateral upslope accumulating (or contributing) area was a first-order control on runoff source area. Additional studies found that hydrologic connectivity is dependent upon antecedent moisture conditions: as moisture decreases, hillslope contributing areas become disconnected from the stream (Jencso et al., 2009; Smith et al., 2013; Nippgen et al., 2015), and the proportion of the catchment area that is hydrologically connected to the stream decreases (D'Odorico and Rigon, 2003; Jencso et al., 2009; Smith et al., 2013; Nippgen et al., 2011, Nippgen et al., 2015). Further complicating the narrative, some uplands have been found to rarely connect to the stream environment at all (Tromp-van Meerveld and McDonnell, 2006), while in some studies, upland signals are dampened or altered by the riparian area near the stream (McGlynn & McDonnell, 2003). Therefore, pairing hydrometric responses with chemical characterizations of source areas ensure the physical plausibility of our end-member mixing analysis and inferences of hydrologic connectivity.

Quantifying hydrologic connectivity relies on the identification of dominant catchment runoff source areas, which can be roughly described in three spatial dimensions: lateral, longitudinal, and vertical (Nadeau & Rains, 2007; Zimmer & McGlynn, 2018). Prior research on lateral hydrologic connectivity has largely been conducted within the context of the variable source area concept (Hewlett & Hibbert, 1967). However, few studies have focused on longitudinal (Godsey & Kirchner, 2014; Phillips et al., 2011; Zimmer & McGlynn, 2018), or vertical (Tague et al., 2008; Zimmer & McGlynn, 2017; Zimmer & McGlynn, 2018) source areas of hydrologic connectivity and even fewer (Covino, 2017; Zimmer & McGlynn, 2018) have considered lateral, longitudinal, and vertical source areas of runoff in concert. To better understand the spatiotemporal variability of streamflow dynamics in a lower elevation montane headwater system, our study pairs geochemical characterization of catchment source areas with hydrometric measurements. We targeted sample collection and measurements to address lateral, longitudinal, and vertical connectivity to a small headwater stream in the Front Range of Colorado, USA. Our holistic approach to quantifying source areas to the stream from differing landscape and topographic features is outlined in a conceptual diagram in Fig. 1. We address the following research questions: 1) what are the dominant sources of streamflow in a small montane headwater stream, and how do they shift in space and time?; and 2) how do landscape topographic features impact dominant source areas?

2. Methods

2.1. Site description

The Manitou Experimental Forest (MEF) is located within the traditional territories of the Cheyenne, and Ute peoples in central Colorado, and has been managed as an Experimental Forest and Range site by the United States Department of Agriculture (USDA) Forest Service's Rocky Mountain Research Station since 1936. Located 48 km northwest of Colorado Springs, the MEF covers 67 km^2, or roughly 2.6% of the Upper South Platte River Basin. The Upper South Platte River Basin serves as a significant water resource, supplying ~50% of the drinking water for the City of Denver (Adams, 2021). The MEF is representative of the montane ponderosa pine zone in the Colorado Front Range, which extends from southern Wyoming to northern New Mexico. The climate is cool (mean temperature is 19 °C in July and −2 °C in January) and dry, with a 20-year annual average precipitation of 304 mm (standard deviation ± 76 mm) (Frank et al., 2021). Precipitation falls as rain during the summer season (June to September), primarily during short-lived convective afternoon thunderstorms characterized by brief but intense periods of rainfall and lightning. Additional precipitation occurs as snowfall from late September to May (Ortega et al., 2014). Snow cover is highly variable in space and time with persistent snowpack on north-facing aspects of the catchment and discontinuous, intermittent snow cover on south-facing aspects. Spring snowmelt pulses can saturate the soil for days to weeks depending on aspect and weather conditions (Berkelhammer et al., 2016).

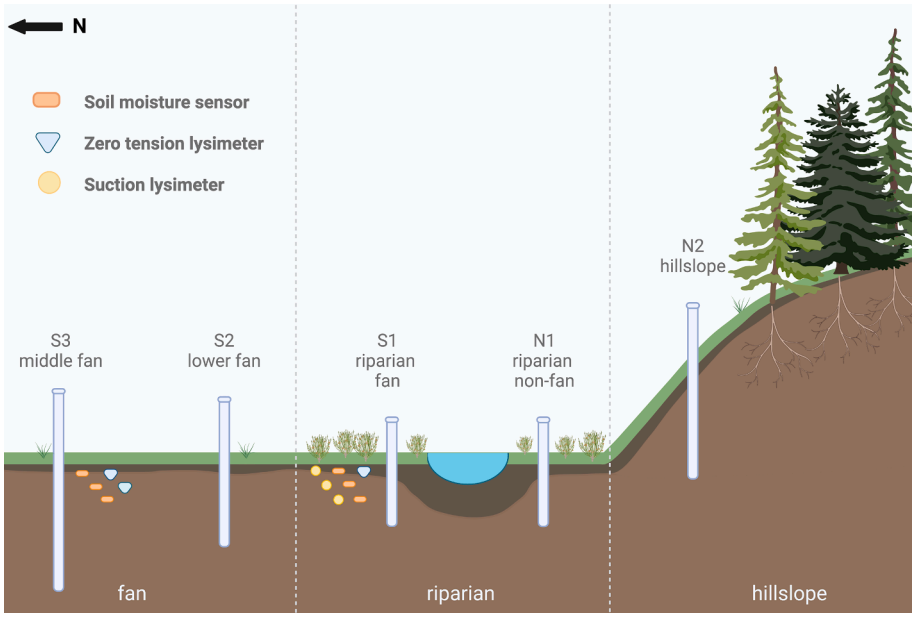

Fig. 1. Conceptual diagram (not to scale) of targeted sample collection and measurements installed within the study area. Created with BioRender.com.

Our study area is a 2.65 km^2 catchment at the headwaters of Hotel Gulch within the MEF boundaries (Fig. 2). Elevation ranges from 2626 m to 2843 m asl. The study area is composed of subcatchments A and B corresponding to different reaches of the stream within Hotel Gulch hereon referred to as Hotel Stream, and their respective drainage areas (Fig. 2, catchment areas and stream lengths are given in Table 1). Reaches of Hotel Stream are non-perennial, drying out through the late summer months and wetting up during spring snowmelt and summer rainstorms.

Forest cover in the area consists primarily of ponderosa pine (*Pinus ponderosa*) mixed with Douglas-fir (*Pseudotsuga menziesii*) generally on south-facing slopes; Douglas-fir on east- and west-facing slopes; Douglas-fir mixed with blue spruce (*Picea pungens*), on north-facing slopes; and quaking aspen (*Populus tremuloides*) mixed with blue spruce, on lower slopes and drainage bottoms (Linkhart, 2001). Steeper, north-facing slopes and higher elevations support mixed Engelmann spruce (*Picea engelmannii*)/Douglas-fir/aspen stands, with lodgepole pine (*Pinus contorta*) appearing on higher ridges (Marchand et al., 2006).

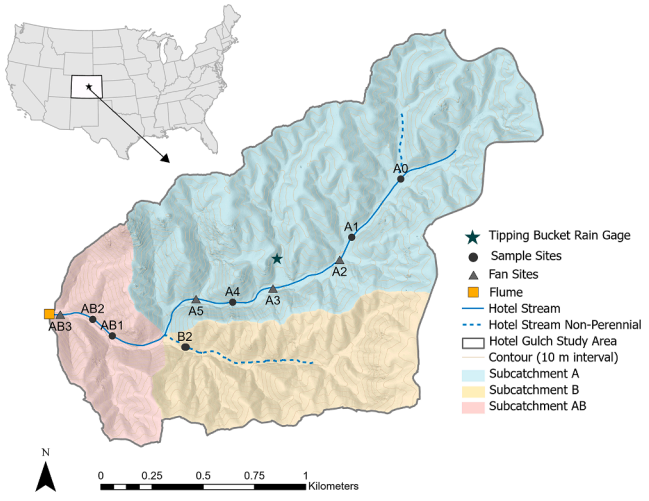

Fig. 2. Location of the Hotel Gulch study area within the Manitou Experimental Forest in central Colorado, USA. Reaches of Hotel Stream were manually sampled and equipped with a level logger to measure stage at sites A0, A2, A3, A5, B2 and AB3. Manual grab samples were also collected from the stream at sites A1, A4, AB1 and AB2. Fan sites A2, A3, A5 and AB3 are instrumented with groundwater wells, soil moisture sensors, and soil lysimeters with increasing lateral distance from the stream (Fig. 1).

Table 1
Catchment areas, lengths of Hotel Stream, and minimum/ maximum elevations of each subcatchment within Hotel Gulch.

Subcatchment	Drainage Area (km^2)	Total Reach Length (km)	Elevation min/ max asl (m)
A	1.63	1.83	2676/ 2828
B	0.65	0.78	2676/ 2819
AB	2.65	3.24	2626/ 2828

The study area is topographically diverse, characterized by steep gulches, rocky outcrops, gently sloping valley bottoms and alluvial/ colluvial fans. Soils are developed from the weakly structured Pikes Peak granite and are highly erodible (Retzer, 1949). The dominant soil orders across the study area are Alfisols and Mollisols, with aquolls found in the riparian zone on either side of the stream (Soil Survey Staff, Natural Resources Conservation Service, United States Department of Agriculture, 2010). Hillslopes have slopes ranging from ~40 to 70%. Hillslope soil profile depths consist of a shallow (0–3 cm) upper organic layer, gravelly coarse sandy loam (~3–23 cm), and a very gravelly loamy coarse sand layer (~23–46 cm) before reaching weathered bedrock (33–155 cm) or bedrock (46–155 cm) depending on the slope with steeper hillslopes having a lower depth to bedrock. Riparian areas and alluvial/ colluvial fans soil profile depths consist of fine sandy loam (0–30 cm), loamy fine sand (30–64 cm), very fine sandy loam (64–127 cm) and coarse sand (127–152 cm) (Soil Survey Staff, 2022). Most soils are poor, with little organic matter (1–4%) except in riparian areas (Retzer, 1949).

2.2. Instrumentation and data collection

A suite of instruments was installed in the study area within Hotel Gulch to characterize seasonal shifts in the longitudinal, lateral, and vertical connectivity between different source areas to Hotel Stream. To better characterize longitudinal stream connectivity, Hotel Stream was sampled along the longitudinal profiles of reach A, non-perennial reach B and reach AB downstream of the confluence between reaches A and B.

Reach A was sampled from the most upstream site of observed persistent, channelized flow along the main stem of Hotel Stream (A0) to just before the confluence with reach B (A5) (Fig. 2). Sites are labeled based on distance from A0 such that sites with higher numbers indicate greater distance from A0. Similarly, sites along reach AB are labeled based on distance from the confluence of reaches A and B. Reach B was sampled from the most downstream observed persistent, channelized flow, B2.

To target instrumentation towards areas with high lateral inputs to Hotel Stream, upslope accumulation area (UAA) was calculated using 1-m resolution airborne laser swath mapping (ALSM) data of our study area courtesy of the National Center for Airborne Laser Mapping-NCALM (Rossi et al., 2022). We used the triangular multiple flow-direction algorithm (MD-infinity) method developed by Seibert & McGlynn (2007) to calculate flow accumulation for our study area [Terrain analyses were completed using the Whitebox Tools plugin for ArcGIS Pro (Lindsay, 2016)). Sites A2, A3, A5 and AB3 were selected for further instrumentation based on UAA (Supplementary Fig. 1). These sites coincide with infrequently activated alluvial/ colluvial fans and are from hereon referred to as fans or fan sites (Fig. 1). Fan sites A3, A5, and AB3 are located on the drier, south-facing aspects while A2 is located on the wetter, more densely vegetated north-facing aspects of Hotel Gulch. To characterize lateral and vertical connectivity of fan sites to Hotel Stream, soil moisture sensors, soil lysimeters, and groundwater wells were installed to differing depths with increased lateral distance adjacent to the stream at each fan site. Soil moisture sensors and soil lysimeters were installed in the shallow subsurface (10-, 30-, 50-cm depths) both adjacent to the stream, and laterally distant from the stream within the fan (Fig. 2). The belowground depth of the groundwater wells varies between 0.6 and 3.7 m with the shallowest groundwater wells nearest to the stream, and the deepest wells furthest from the stream.

2.3. Hydrometric measurements

2.3.1. Streamflow and precipitation

Stream stage data were recorded every 5 min at the most upstream site (A0), adjacent to each fan site (A2, A3, A5, and AB3), and at the outlet of the non-perennial reach B (B2) using capacitance water level loggers (Odyssey Dataflow Systems Limited) in 2019 and 2020, and a pressure transducer (Onset HOBO U20L-04 Water Level Data Logger) in 2021. Stage data were converted to specific discharge using a rating curve based on a minimum of fifteen salt dilution measurements per site following Moore (2004). Rainfall data were recorded every 5 min using a tipping bucket rain gauge (TR-525M, Texas Electronics, Dallas, TX) installed at site A3 (Fig. 2). Rainfall samples were collected following rainstorms in a bulk rainfall collector installed adjacent to the tipping-bucket rain gage at site A3, clear of canopy cover in all directions. The rainfall collector consisted of a funnel and tube fed into a HDPE bottle supplied with mineral oil and sealed with putty to prevent evaporation and dust inputs. Snow core samples were collected monthly between November 2019 and April 2021. Snow water equivalent (SWE) and snow depths were estimated for our study area using the Snow Data Assimilation System (SNODAS) (National Operational Hydrologic Remote Sensing Center, 2004). SNODAS is a daily, 1-km^2 resolution modeled snow product available for the contiguous U.S. provided by the National Oceanic and Atmospheric Administration (NOAA) National Weather Service's National Operational Hydrologic Remote Sensing Center (NOHRS). Snowfall totals for each year were obtained from the Community Collaborative Rain, Hail and Snow Network (CoCoRaHS; Reges et al., 2016) from a monitoring site in Woodland Park, CO approximately 13 km from the study area.

2.3.2. Groundwater

To monitor lateral connectivity between the landscape and the stream, we installed groundwater wells with increasing distance from the stream within the selected fan sites (Fig. 1). Each site has between 4 and 6 groundwater wells: 3 to 4 on the fan side of the stream including one in the riparian zone (within near-stream riparian vegetation) hereon referred to as riparian fan, one within the fan but outside of the riparian zone (lower fan), and at least one further upland (middle fan). Due to the larger size of the fan at site A3, we installed an additional fan well, so there are four total wells within the fan at this site with the furthest labeled upper fan. All fan sites have at least one groundwater well on the non-fan side of the stream (riparian non-fan). The lower fan sites AB3 and A5 have an additional non-fan groundwater well installed outside of the riparian zone just beyond the toe-slope break (hillslope) (Fig. 1). Due to rocky terrain and steep hillslopes, we were unable to install hillslope wells at the upper fan sites. Groundwater wells installed on roughly south-facing aspects are labeled "S", while those installed on roughly north-facing aspects are labeled "N". Wells are numbered according to distance from the stream such that well names ending in "1" were installed closest to the stream, while those ending in "3" (or "4" in the case of site A3) are furthest from the stream (see Fig. 1, Table 2). Distances between groundwater wells and the stream vary at each fan site depending on the location of riparian vegetation, and where subsurface saturation could be reached using a 4.6 m hand auger. Information on groundwater wells installed at each site can be found in Table 2. All wells were screened over their entire length and were backfilled with washed sand and sealed at the surface with a thin layer of bentonite clay. Groundwater levels were recorded with a pressure transducer every 5 min in riparian wells for all study years and at all wells during the 2020 and 2021 field seasons (Onset HOBO U20L-04 Water Level Data Logger). The logger for A2N3 was damaged during the winter of 2020 and was not deployed during the 2021 study season. Groundwater levels remained below the depth of our groundwater well at AB3S3 resulting in no level data for that site, and the logger was subsequently removed in mid-August of 2020.

2.3.3. Soil moisture

Volumetric water content (VWC, %) data were recorded by soil moisture sensors (Acclima TDT Digital Sensor ACC-SEN-SDI) installed adjacent to each riparian well ($VWC_{riparian}$), and at the groundwater well furthest from the stream on the fan side of the stream at each site (VWC_{upland}) (Fig. 1) at sites A2, A3, A5 and AB3. $VWC_{riparian}$ and VWC_{upland} sensors were installed at 10-, 30- and 50- cm depths except for $VWC_{riparian}$ at site A3, where the sensors were installed at 10, 20 and 35 cm depths due to the presence of the water table at 50 cm. Acclima TDT sensors can resolve 0.06% changes in VWC; the typical absolute VWC accuracy is around 2%.

2.4. Geochemical characterization

2.4.1. Stream chemistry

Stream samples were collected approximately weekly from the start of snowmelt in early May through the end of October between 2018 and 2020, and monthly in 2021. Stream sample sites between fan sites (A1, A4, AB1, AB2) were sampled less frequently and mainly during the 2018 and 2019 study years. Certain sites remained frozen through spring and were the first to freeze in early fall (A3, A5, B2) and were subsequently sampled less frequently. Portable automatic samplers were installed at select fan sites (sites A3, A5, AB3) during the summer months of 2019, 2020 and 2021 to automatically collect daily stream samples (model-6712, Teledyne ISCO, Lincoln, NE, USA).

2.4.2. Groundwater and soil water chemistry

To better characterize hydrologic connectivity between the fans and the stream, groundwater and soil water were collected approximately weekly from May through October between 2018 and 2020 and monthly in 2021. Groundwater wells were purged with a bailer and allowed to recharge before sample collection. To characterize soil water chemistry, soil water lysimeters were installed adjacent to each soil moisture sensor nest (Fig. 1). Suction lysimeters (PRENART Super Quartz samplers and

Table 2
Drainage area, aspect, soil water, and groundwater well information for each fan site within the Hotel Gulch study area.

Site	Drainage Area (km^2)	Aspect	Site Wells	Well Positions	Soil moisture/ Soil Lysimeter Depths (cm)	Distance from Stream (m)	Depth Belowground (m)
A2	0.88	North	A2S1	Non-fan riparian	–	4.1	1.0
			A2N1	Riparian fan	Suction (S): 10, 30, 50 0-Tension: 10 VWC: 10, 30, 50	3.6	1.0
			A2N2	Lower fan	–	14.2	1.0
			A2N3	Middle fan	0-Tension: 10, 30 VWC: 10, 30, 50	21.2	2.1
A3	1.20	South	A3S1	Riparian fan	Suction (S): 10, 20, 35 0-Tension: 10 VWC: 10, 20, 35	3.7	1.2
			A3N1	Non-fan riparian	–	4.2	1.0
			A3S2	Lower fan	–	17.7	1.9
			A3S3	Middle fan	–	41.5	2.6
			A3S4	Upper fan	0-Tension: 10, 30 VWC: 10, 30, 50	59.6	3.8
A5	1.47	South	A5S1	Riparian fan	Suction (S): 10, 30, 50 0-Tension: 10 VWC: 10, 30, 50	4.8	0.8
			A5N1	Non-fan riparian	–	4.9	1.2
			A5S2	Lower fan	–	30.1	3.8
			A5S3	Middle fan	0-Tension: 10, 30 VWC: 10, 30, 50	63.9	1.9
			A5N2	Hillslope	–	18.5	2.0
AB3	2.65	South	AB3S1	Riparian fan	Suction (S): 10, 30, 50 0-Tension: 10 VWC: 10, 30, 50	2.8	0.7
			AB3N1	Non-fan riparian	–	2.3	0.7
			AB3S2	Lower fan	–	10.2	1.2
			AB3S3	Middle fan	0-Tension: 10, 30 cm VWC: 10, 30, 50 cm	12.9	1.3
			AB3N2	Hillslope	–	5.2	2.8

Polypropylene collecting bottle/vacuum containers) were installed at 10-, 30-, and 50-cm depths at riparian sites A2, A5, and AB3. Riparian suction lysimeters were installed at 10-, 20-, and 35-cm depths at site A3 due to the presence of the water table. Zero-tension lysimeters were installed to capture preferential/subsurface flow through the soil matrix at 10 cm at the site closest to the stream and at 10 and 30 cm at the site furthest from the stream. Zero tension lysimeters could not be installed deeper than 10 cm near the stream due to the presence of the water table. Zero-tension lysimeters consisted of a small funnel filled with wash sand installed and backfilled within the soil profile connected to a tube and a 1-L HDPE collection bottle.

2.5. Chemical analysis

Stream, soil water, groundwater, and precipitation samples were filtered through glass microfiber filters (Whatman: glass microfiber filters, Grade GF/F) within 24 h of collection. Ion chromatography (Dionex Aquion Ion Chromatography System) was used to analyze all samples for major cations (Ca, Na, Mg, K) and major anions (Cl, SO_4, NO_3). Duplicates were analyzed on 10% of all samples to ensure precision and known standards and analytical blanks were run during each analysis to verify accuracy (± 2.5% from known values).

2.6. Analytical methods

2.6.1. Hydrologic seasons

To investigate potential drivers of temporal shifts in hydrologic connectivity between fans and Hotel Stream, we analyzed observed precipitation data collected at the Manitou Experimental Forest meteorological station (located ~5 km from the rain gage installed at site A3 of our study area). Given that Hotel Stream remains frozen from November through late April, and most of our samples were collected from early summer to early fall, we focused our precipitation analysis on 20-year observed rainfall data between May and October (Frank et al., 2021). Using average daily rainfall totals from the 20-years prior to our study, we separated our analysis into three distinct hydrometric periods: May to mid-June [approximate day of year (DOY) 121 – 175] characterized by low-intensity rainfall where streamflow is dominated by snowmelt, mid-July to mid-August having sporadic high-intensity rainfall inputs (DOY 176 – 223), and mid-August through the end of October with little to no rainfall (DOY 224-305) (Fig. 3). These periods roughly correspond to observed trends in streamflow in similar Front Range catchments, where snowmelt causes high streamflow in the spring, followed by a steady decrease in streamflow interrupted sporadically by summer thunderstorms, and a return to baseflow in late summer to fall (e.g., Bukoski et al., 2021, Cowie et al., 2017). Therefore, we focused our analysis on these three distinct hydrologic seasons: melt out during spring, wet-up during summer rainstorms, and a return to baseflow in fall.

2.6.2. End-member mixing analysis

To identify source areas of longitudinal, lateral, and vertical stream connectivity, the chemical dataset collected from Hotel Gulch was used in principal component analysis (PCA) and EMMA following the methods of Christophersen and Hooper (1992). Source areas, or potential end-members, for each fan site considered in EMMA included: stream water from the nearest longitudinally upstream stream site (upstream A or upstream B), groundwater collected with increasing lateral distance from the stream within the fan (riparian fan, lower fan, middle fan, upper fan), or the non-fan side of the stream (riparian non-fan or hillslope), soil water collected from riparian suction lysimeters (S) or from riparian or fan zero tension lysimeters (0-Tension). EMMA was completed for all collected stream samples at each fan site following the methods of Christophersen and Hooper (1992). Tracer selections and end-member mixing scenarios were based on criteria adapted from Christophersen and Hooper (1992), while also incorporating the results of our hydrometric characterizations. All analyses were performed using the R 4.2.0 statistical programming language (R Core Team 2022).

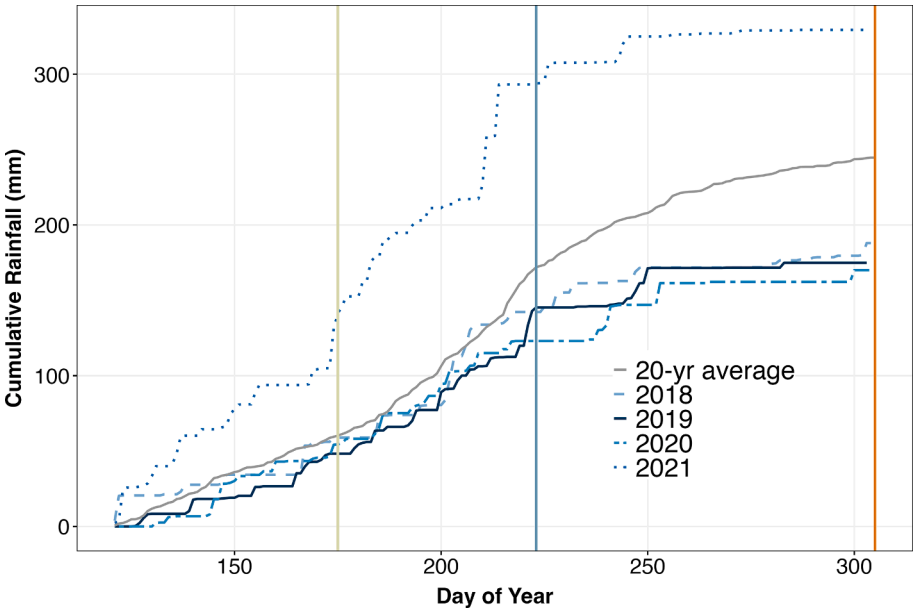

Fig. 3. Cumulative daily rainfall collected in Hotel Gulch from 2019* to 2021, compared to the observed 20-year average collected from the Manitou Experimental Forest (MEF) headquarters meteorological tower (solid gray line). The green (first) vertical line indicates the end of the spring hydrologic season, the blue (second) the end of the summer, and the orange (third) the end of the fall. *The Hotel Gulch tipping bucket was not installed until 2019; data from 2018 were collected at the MEF headquarters meteorological tower. (For interpretation of the references to colour in this figure legend, the reader is referred to the web version of this article.)

Tracers were selected from the whole stream data set from solutes which were consistently found at detectable levels in streamflow: Cl, F, SO_4, Mg, Ca, Na, and K. Significant outliers were defined as any data point more than two standard deviations above or below the mean of the data and were removed from analysis to prevent outliers (resulting from geochemical anomalies or analytical errors) from having a disproportionate influence on results. Tracers were selected based on: (i) ability to distinguish between end-members, (ii) maximation of the percent of variance in each stream dataset explained by the first two principal components (PC1, PC2), and (iii) consistency with the conservative mixing hypothesis. Regarding the first criterion, we tested if the mean concentrations of each solute were significantly different ($p < 0.05$) among at least one pair of potential end-members using a Tukey-Kramer test (Tukey HSD test in the "agricolae" R package). For the second, eigenvectors (calculated in PCA) were summed to ensure the majority of variance was explained by PC1 and PC2. Lastly, we created bivariate scatter plots of solutes to ensure that those selected do not co-vary in an apparent non-linear fashion, which would indicate non-conservative mixing (uptake or release). We selected solutes with Pearson's correlation r^2 values > 0.5 with p-values < 0.01 as tracers.

2.6.3. Stream chemistry and mixing models

To characterize spatiotemporal shifts in stream water chemistry, we generated mixing scenarios projected in principle component space corresponding to each fan site within each hydrologic season described above. The stream water solute data set were standardized by centering them about their means and dividing them by their respective standard deviations. Standardizing stream chemistry data in this way ensures that solutes with the greatest variability do not have more influence on the mixing model. Principal component analysis (PCA) was performed on each standardized stream dataset to determine the dimensionality, or the rank order, of the dataset. The number of principal components retained in the mixing model was determined by plotting the eigenvectors for each rank order in a scree plot (Cattell, 1966). Within the scree plot, smaller eigenvectors represent random variation in the dataset, and tend to lie along a straight line. The point where the first eigenvector departs from this line distinguishes the non-random variation in principal components, indicating the number of components, or end-members, to retain.

2.6.4. End-member selection and relative contributions

After the number of end-members required for each mixing space was defined, we examined the potential source areas within each fan site to assess their ability to explain the chemical composition of stream water. For each hydrologic season, end-member concentrations were standardized by subtracting the means and dividing by the standard deviation of the stream observations. End-member concentrations were then projected into each mixing space by multiplying the standardized values by the matrix of retained eigenvectors from the stream PCA for visual inspection of each potential mixing scenario. End-members were selected based on the following criteria: (i) ability to effectively explain variation in stream chemistry such that all or most stream samples can be represented as a mixture of two or more end-members and (ii) agreement with hydrometric data such that end-members which do not appear hydrologically connected to the stream based on our hydrometric dataset do not represent stream connectivity with that source area.

To determine the relative proportions of stream runoff derived from retained end-members, hydrograph separations were completed on each stream solute dataset using the standard simultaneous equations for two (Equations (1) – (2)) and three (Equations (3) – (5)) end-member mixing models with principal components one and two as tracers:

$$f_1 = \frac{\left(PC^1_{stream} - PC^1_2\right)}{\left(PC^1_1 - PC^1_2\right)} \tag{1}$$

$$f_2 = 1 - f_1 \tag{2}$$

$$f_1 = \frac{\left(PC^1_{stream} - PC^1_3\right)\left(PC^2_2 - PC^2_3\right) - \left(PC^1_2 - PC^1_3\right)\left(PC^2_{stream} - PC^2_3\right)}{\left(PC^1_1 - PC^1_3\right)\left(PC^2_2 - PC^2_3\right) - \left(PC^1_2 - PC^1_3\right)\left(PC^2_1 - PC^2_3\right)} \tag{3}$$

$$f_2 = \frac{\left(PC^1_{stream} - PC^1_3\right)}{\left(PC^1_2 - PC^1_3\right)} - \frac{\left(PC^1_1 - PC^1_3\right)}{\left(PC^1_2 - PC^1_3\right)} f_1 \tag{4}$$

$$f_3 = 1 - f_1 - f_2 \tag{5}$$

where f_x is the fractional contribution of end-member x to streamflow, and PC^i_x is principal component i of end-member x. In some cases, stream observations happened to lie outside the mixing domain defined by the selected end-members, resulting in negative fractions of relative contributions (Liu et al., 2004). In this case, negative fractions were forced to zero and other contributions were assumed to be a mixture of the

remaining end-members only (Liu et al., 2004).

Results of each end-member mixing scenario were tested based on their ability to reproduce original stream solute values by multiplying end-member fractions by the original mean end-member solute concentrations. Mixing model fitness was quantified using simple linear regression between observed and back-calculated stream solute concentrations, with mixing model fitness as the coefficient of determination (R^2) between original and reproduced stream solute values.

3. Results

3.1. Meteorological context

Compared to the 20-year average rainfall recorded between May and October at the MEF headquarters meteorological station (Frank et al., 2021), 2021 was wetter-than-average, and 2019 and 2020 were drier-than-average years (Fig. 3). Rainfall totals in 2021 were 135% of the 20-year May through October average, while 2019 and 2020 were 71% and 69% of the 20-year average, respectively (Table 3). The Hotel Gulch tipping bucket rain gage was not installed until 2019, so we do not have data comparisons between our study area and the 20-year rainfall record for 2018. However, rainfall totals collected at the MEF meteorological station data for 2018 were 77% of the 20-year rainfall record.

Among each hydrologic season, summer of 2021 had the highest rainfall totals, followed by summer of 2019, 2018 and 2020. Spring rainfall was also highest during the 2021 study year, followed by 2018, 2020 and 2019. Fall rainfall was highest in 2020, followed by 2018, 2021 and 2019 (Table 4).

SNODAS derived estimates of snow depth were lowest in 2018 with an estimated average depth of 164 mm, and highest in 2021 with an estimated average depth of 456 mm. Snow depth was estimated at 383 mm in 2019, and 299 mm in 2020. SNODAS derived estimates of peak snow water equivalent (SWE) averaged for the study area was 20 mm in 2018, 55 mm in 2019, 49 mm in 2020 and 64 mm in 2021 (Table 3). The 2021 study year received both more rain and had higher average SWE, making it a wetter-than-average year compared to the other study years.

3.2. Hydrometric response of fan sites

3.2.1. Streamflow and precipitation

Streamflow varied among sites and study years. Site A5 exhibited frequent intermittency in streamflow, particularly from late June, July, and August of 2020, making comparisons between streamflow and lateral contributions to the stream difficult to quantify at this site. For this reason, we focus the remainder of the lateral and vertical connectivity analysis on fan sites A2, A3, and AB3. Observed trends in the hydrometric dataset were similar across all fan sites. Because of this, data for site A3 are shown in Fig. 4 while data for sites A2 and AB3 are available in the Supplementary Material (Supplementary Figs. 2 & 3). Across all sites, the 2019 and 2020 study years had lower streamflow than that during 2021. This relationship between wet and dry years corresponded to the precipitation totals for each year with the lowest snowpack and rainfall totals measured in 2020, and highest in 2021, with 2019 rainfall totals falling between the two (see Table 3, and daily rainfall totals in Fig. 3). Streamflow exhibited a similar pattern to the observed rainfall recorded at the MEF headquarters meteorological tower with highest flows in spring and a continual decrease in flow with short interruptions from summer rainstorms (Fig. 4, Supplementary Figs. 2 & 3). Streamflow was most responsive to the high-intensity rainstorms occurring in late July to early August of 2020 and 2021, and prolonged rainfall occurring in early September of 2019 (Fig. 4).

Daily average specific discharge (discharge values recorded at each site divided by the site catchment area given in Table 2) increased with increasing distance downstream (gaining) along reach A (sites A2, A3) during the entire 2019 study period (Fig. 5). During 2020, reach A switched from gaining to decreasing with increasing distance downstream (losing) between sites A2 and A3 on May 31st (DOY 151), and remained losing until the end of the study period in 2020. In 2021, reach A routinely switched from gaining to losing from early May through late June (DOY 181) but switched to losing from A2 to A3 during peaks in streamflow from June 24th (DOY 175) to August 13th (DOY 225). The stream was generally losing from reach A to reach AB, except during the beginning of the 2020 study period when it was gaining from early May until the end of June (DOY 181).

3.2.2. Groundwater and soil moisture

Groundwater levels exhibited little response to rainfall inputs except for during the 2021 wet year (Fig. 4). Specifically, all groundwater well levels increased during the high intensity rainstorms in late June and early August of 2021, with a higher response recorded in wells closer to the stream. During this storm, the largest fan response was recorded at site A3 with A3S2 and the lowest response was recorded at the furthest groundwater well at site A3S4. In general, the non-riparian groundwater wells installed within the uplands of the fans (S2 – S4 or N2 – N3) were less responsive compared to the riparian groundwater wells (S1 or N1). All groundwater levels exhibited a decline from spring to fall. This decline was prominent at upland groundwater sites, and groundwater levels at certain sites declined below the depths of our groundwater wells causing our wells to dry down. At site A2, A2N3 dried down as early as June 24, 2020 (DOY 175), A2N2 dried down starting on August 13, 2020 (DOY 225), and September 12, 2021 (DOY 255) (Supplementary Fig. 2). At site A3, A3S4 dried down on October 29, 2020 (DOY 302) and A3S3 dried down starting on August 13, 2020 (DOY 225), and October 22, 2021 (DOY 295) (Fig. 4).

At all sites, $VWC_{riparian}$ and VWC_{upland} were most responsive during the 2021 study year. Within each site, $VWC_{riparian}$ was generally higher across all depths compared to VWC_{upland} at any depths. Across all sites and all depths, $VWC_{riparian}$ ranged between 5 and 80%, with site A2 having the lowest values recorded at 10- and 30-cm depths. Across all sites, the deepest $VWC_{riparian}$ depth remained relatively constant, ranging between 40 and 50%. VWC_{upland} across all sites and depths ranged from 0 to 30% with driest conditions measured at site A2, and

Table 3
Rainfall totals from May through October for the years of study collected at the tipping bucket rain gage at site A3 compared to the May through October 20-year rainfall total average collected at the Manitou Experimental Forest (MEF) Headquarters (HQ) meteorological station (245 mm; standard deviation ± 63 mm). The Hotel Gulch rain gage was installed in 2019; 2018 rainfall data compare MEF HQ rainfall totals to the 20-year observed average. Snowfall totals from November through April of each water year were collected from Woodland Park (CoCoRaHS). Snowpack data were collected at site A3 using trail camera imagery for 2020 and 2021 and estimated using SNODAS for 2018 and 2019. Peak SWE totals were derived using SNODAS data.

Study Year	Hotel Gulch Rainfall Totals (mm)	Observed Average Rainfall Totals (%)	Snowfall Totals (mm)	Average Peak Snow Depth (mm)	Average Peak SWE (mm)
2018	188	77	1024	164	20
2019	175	71	1318	383	55
2020	170	69	1801	299	49
2021	330	135	1090	456	64

Table 4
Rainfall totals of each hydrologic season for each study year.

Study Year	Spring Rainfall Totals (mm)	Summer Rainfall Totals (mm)	Fall Rainfall Totals (mm)
2018	59	83	46
2019	48	97	30
2020	54	69	47
2021	141	153	35

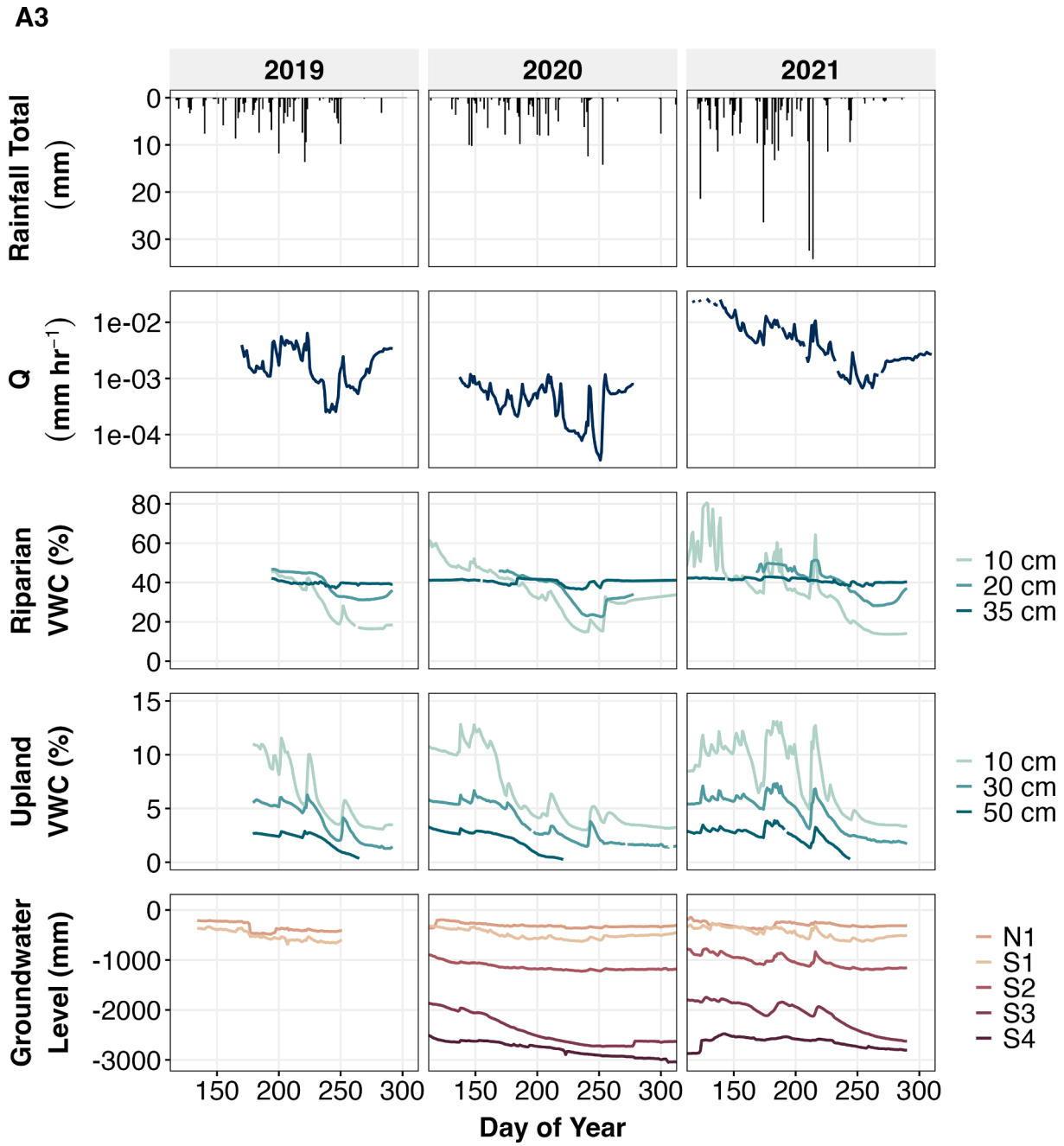

Fig. 4. Hydrometric time series data for site A3 with daily rainfall totals (mm), log-transformed daily average specific discharge (mm hr^{-1}), daily average volumetric water content (VWC, %) at riparian and upland sites, and daily average groundwater levels (mm). Groundwater levels correspond to riparian wells on north-facing (N1) and south-facing (S1) sides of the stream, and non-riparian wells installed with increased lateral distance from the stream (S2 – S4) within fan site A3. Hydrometric time series for sites A2 and AB3 can be found in Supplementary Figs. 2 & 3.

wettest conditions measured at site A3. As with groundwater levels, we observed a decline in VWC across all sites and depths at both upland and riparian positions (Fig. 4, Supplementary Figs. 2 & 3).

3.3. Geochemical response

3.3.1. Stream chemistry

Stream solute concentrations did not appear to be influenced by shifts in gaining-losing discharge dynamics along the longitudinal stream profile during any of the study years (Fig. 5). Rather, stream solute concentrations appear to shift on a seasonal scale. Temporal variation in stream solute concentrations of Mg, Na, and Ca exhibited a pattern of decreased concentrations likely from snowmelt during the spring, followed by increased concentrations during the summer months (Fig. 5). For example, Ca concentrations increased ~6.0 mg L^{-1} at sites A2 and A3, and 3.0 mg L^{-1} at AB3, with values starting at roughly 13.0 mg L^{-1} in spring. Conversely, stream solute concentrations of Cl, K, and SO_4 exhibited increased concentrations in the spring with either decreased, or relatively constant concentrations during the summer months depending on the site (Fig. 5). At sites A2 and A3, Cl, K, and SO_4 concentrations decreased from spring to summer, and returned approximately to spring concentrations during the fall. However, at site AB3 concentrations varied between study years and temporal patterns were more difficult to discern. For example, Cl generally decreased from roughly 1.2 to 0.8 mg L^{-1} in 2019 and 2021 but fluctuated between ~1.3 and 1.0 mg L^{-1} in 2020. F was generally less variable than other solutes,

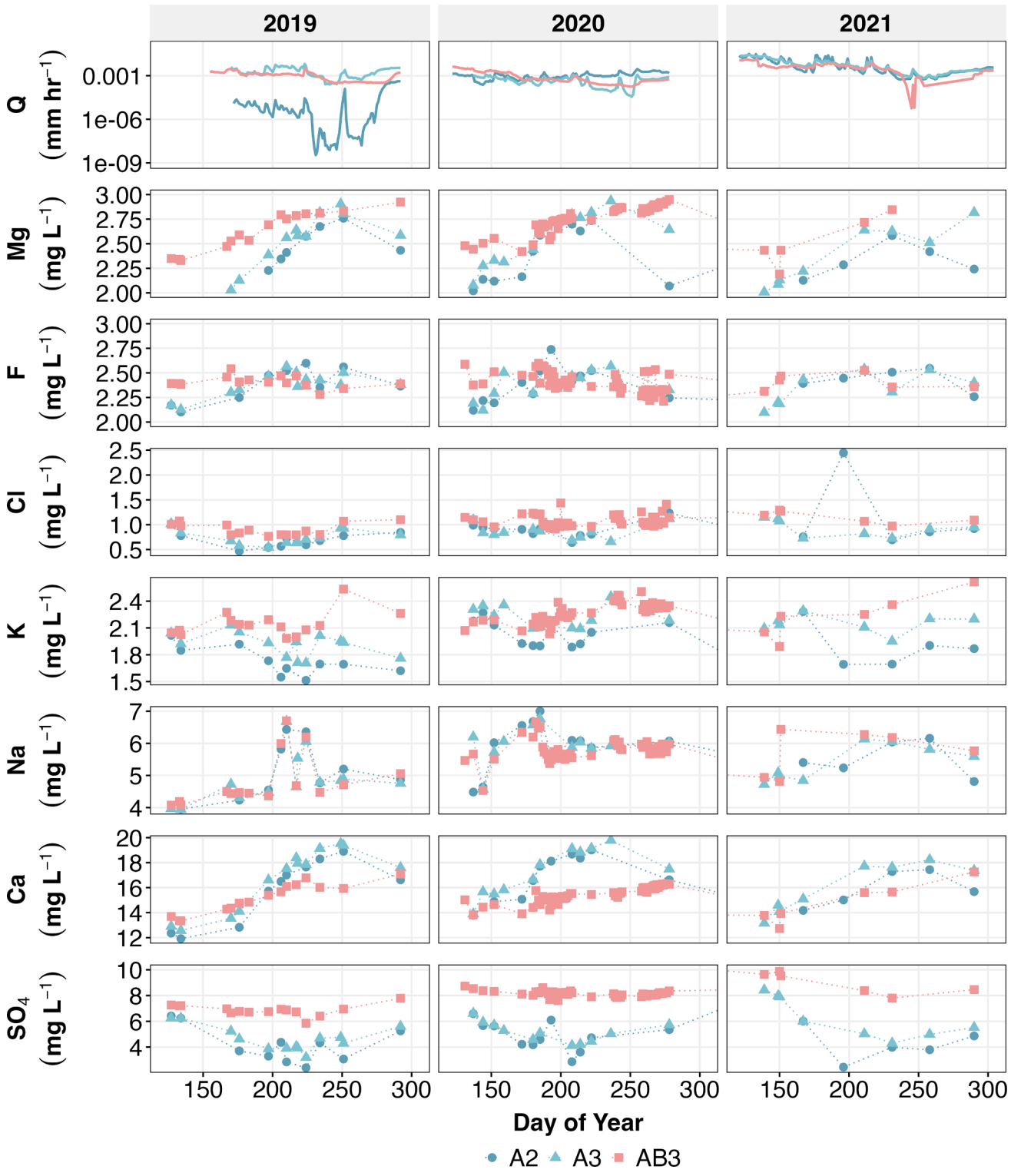

Fig. 5. Log-transformed daily average specific discharge (mm hr^{-1}) and solute concentrations in mg L^{-1} during the 2019, 2020 and 2021 study years for fan sites A2, A3 and AB3. During the 2020 study season, daily stream samples were collected using an autosampler at site AB3, and subsequently has more data points than sites A2 and A3.

varying between roughly 2.2 and 2.5 mg L^{-1} across sites and seasons.

Solute concentrations aggregated across all study years varied along the longitudinal stream profile, generally increasing with increased distance from the headwater (Fig. 6, Supplementary Table 1). Compared to reach A, reach B had higher concentrations of all solutes except for Na, which did not have a distinguishable longitudinal pattern. As a mixture of reaches A and B, reach AB had the second highest concentrations for all solutes. Certain solutes exhibited distinct differences among hydrologic seasons (Fig. 6, Supplementary Table 1). This was particularly pronounced when comparing spring against summer and fall hydrologic seasons, with higher spring concentrations for SO_4 and Cl, and lower concentrations for K, F, Mg, Ca, and Na.

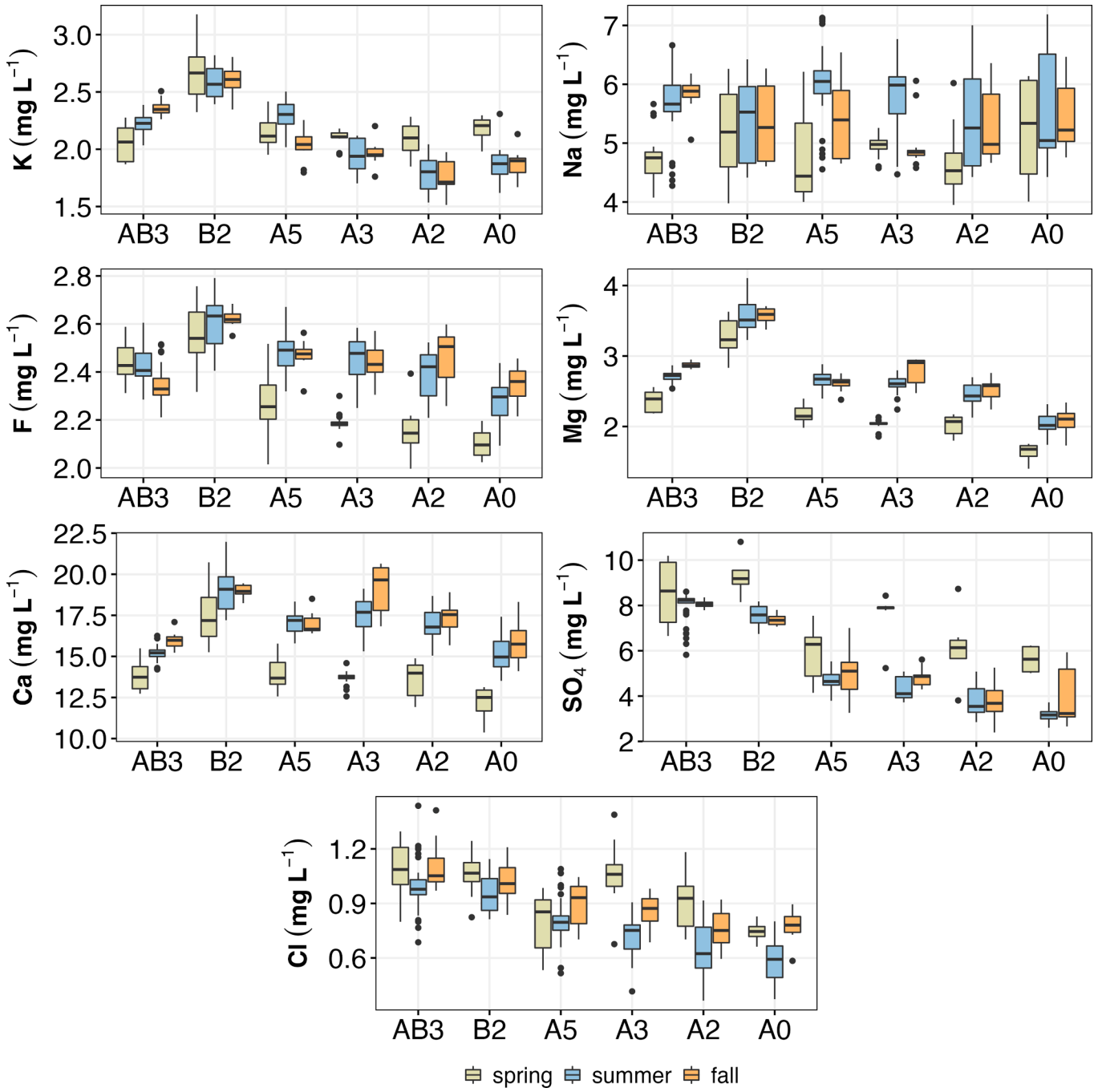

Fig. 6. Solute concentrations (mg L^{-1}) along the longitudinal stream profile collected during spring, summer, and fall hydrologic seasons from 2018 through 2021. One non-statistical outlier was removed from the spring chloride boxplot for site A0 (8 mg L^{-1}) for better visualization of longitudinal trends. Sample counts and mean and standard deviation values for solute concentrations can be found for the entire longitudinal stream profile in Supplementary Table 1.

3.3.2. Groundwater and soil water chemistry

Groundwater and soil water solute concentrations varied with distance from the stream, depth, and hydrologic season across sites (Supplementary Tables 2–4). Groundwater concentrations of Mg, Na, Ca, K and SO_4 generally increased with increasing distance from the stream for each site. This was particularly pronounced during the fall; at site A3, mean stream SO_4 concentration was 4.8 mg L^{-1}, while mean upper fan groundwater was 15.3 mg L^{-1}. Riparian fan groundwater concentrations of Mg, Na, and Ca were generally lower than that of the stream across all seasons. In addition, all solutes except for Na where higher in the non-fan riparian groundwater compared to the riparian fan groundwater. This was most pronounced at site A2 during the fall season where mean Ca concentration was 37% higher in riparian non-fan groundwater compared to riparian fan groundwater.

Generally, soil solute concentrations were highest at the deepest riparian suction lysimeter depth. The highest mean soil solute concentration was measured during the fall from 50 cm at site A2. Notably, mean Ca was 44.5 mg L^{-1}, mean Mg was 6.4 mg L^{-1}, and mean Na was 10.5 mg L^{-1}. Soil water collected using zero-tension lysimeters was generally more dilute compared to the suction soil water (Supplementary Tables 2–4). This dilution likely reflects infiltration of precipitation with short contact time with the soil.

3.4. End-member mixing analysis

3.4.1. Stream water chemistry and selection of stream tracers

Tracers were selected by applying the previously described criteria to the whole stream data set across all hydrologic seasons. Bivariate plots of major stream solutes revealed significant relationships ($r^2 > 0.5$, $p < 0.01$) for K, Mg, F, and SO_4 for reach A and Mg, Cl, and SO_4 for reach AB, making them suitable tracers for analysis. Sodium (Na) appeared to be an important tracer for reach AB given our thresholds for significance but was not selected due to its apparent non-linear behavior exhibited in Supplementary Fig. 4. The selection of K and F as tracers for stream reach A is consistent with those suggested by Gregory et al. (2022) for the Hotel Gulch study area. Selected tracers were used across each hydrologic season for each site.

3.4.2. Selection and nature of end-members

An independent mixing space dimensionality analysis was performed for each stream water geochemical dataset associated with each hydrologic season (Fig. 7). Of the nine spatiotemporal scenarios analyzed, five required two end-member mixing scenarios and the remaining four required three end-member mixing scenarios. The spring hydrologic season required two end-members for every site. All hydrologic seasons required two end-member mixing scenarios at site AB3. The range in percent variance explained by the first two principal components (PC1 and PC2) for the two end-member mixing scenarios ranged from 85 to 97% while that for three end-member mixing scenarios ranged from 90 to 95%.

When projected into principal component (PC) space, stream samples at all sites during the spring season were best explained by a mixture of upstream A chemistry and one groundwater source (non-fan riparian, upper fan, and riparian fan for sites A2, A3 and AB3 respectively). This agrees with our hydrometric data, as groundwater well levels are highest during spring melt out (Fig. 3). During the summer season, stream samples at A2 were best explained by a mixture of riparian suction lysimeter soil water [riparian soil (S)] at 50 cm, riparian non-fan groundwater, and upstream A chemistry. At site A3, stream chemistry was best explained by upstream A, riparian non-fan groundwater and riparian soil (S) at 35 cm. Moving downstream to site AB3, stream chemistry was best explained by upstream A and lower fan groundwater chemistry. The inclusion of riparian soil (S) at 50 cm for site A2 and 35 cm for site A3 aligns with our hydrometric measurements of soil moisture, as $VWC_{riparian}$ at these depths remains saturated at each site across all study years (Fig. 3, Supplementary Fig. 2). In addition, our hydrometric data confirm that the riparian non-fan groundwater wells at sites A2 and A3 remain hydrologically active throughout each summer. Despite appearing to best explain the stream mixing scenario in PC space, the middle fan groundwater well at site A2 dries down during the late summer months of each study year (Supplementary Fig. 2) and therefore, was not selected as an end-member. Lastly, during the fall season the stream chemistry is best defined by upstream A, riparian soil (S) at 50 cm and riparian soil (S) at 30 cm for site A2, upstream A, lower fan groundwater and riparian fan groundwater at site A3, and upstream B and lower fan groundwater at site AB3. As during the summer season, the inclusion of riparian soil at 30- and 50 cm for site A2 and 35 cm for site A3 aligns with our observation of continued saturation at these depths.

3.4.3. Relative proportion of contributions across space and hydrologic seasons

Contributions from upstream chemistry were highest during the spring season, and lowest during the fall season for each site. The majority of groundwater contributions across all spatiotemporal mixing scenarios were from the lower fan, riparian fan, and riparian non-fan groundwater wells. At site AB3, riparian fan groundwater and lower fan groundwater chemistry contributed to approximately half of the stream chemistry for each season. At site A3, riparian non-fan groundwater contributed to 22% of the stream chemistry during the summer, and the lower fan groundwater contributed to 42.9% of the stream chemistry during the fall. At site A2, riparian non-fan groundwater contributed to 17.3% of the stream chemistry in the spring and 19.7% during the summer. The only exception occurred at site A3 during the spring season where upper fan groundwater contributed 21.9% of the stream chemistry. Sites A2 and A3 appear to become disconnected from groundwater further from the stream and more connected to riparian source areas through time. Surprisingly, upstream B does not contribute chemically to site AB3 until the fall season.

3.4.4. Evaluation of EMMA results

R^2 values between observed and back-calculated stream solute concentrations were variable, ranging from 0.10 to 0.99, with the majority of slopes near one (Table 5). Instances where slopes strayed from unity between observed and back-calculated concentrations indicate that the models may lead to over or under prediction of the observed concentrations of certain solutes. Slopes furthest from unity were found at site A2 during the fall season with 5.02 for Mg, and 0.11 for K. R^2 values were particularly weak (< 0.2) during the fall season at sites A2 and A3 for tracers Mg, F, and K, and during the summer at site A2 for K.

4. Discussion

Using a combined approach of hydrometric monitoring and end-member mixing analysis, we assessed hydrologic connectivity of a small headwater catchment within the Colorado Front Range. Focusing on alluvial/ colluvial fans corresponding to areas with high upslope accumulation area (UAA), we characterized the geochemistry and hydrometric responses of source areas contributing to streamflow in three dimensions: lateral, longitudinal, and vertical. The results of our hydrometric characterizations of soil moisture and ground water levels (Fig. 4, Supplementary Figs. 2 & 3) and EMMA (Fig. 7) indicate that source areas to the stream shift in space and time in this montane headwater catchment. We found that the longitudinal signal from upstream sites became less important than lateral contributions among our defined hydrologic seasons of spring, summer, and fall.

4.1. Lateral, longitudinal, and vertical source areas to the stream shift with distance downstream and between hydrologic seasons

The main contributors to site specific (local) streamflow were upstream surface water and local groundwater. The majority of lateral source areas between the fan sites and Hotel Stream ranged from shallow subsurface riparian soil pore water collected between 30 and 50 cm, riparian groundwater (fan and non-fan) ranging from 0.7 to 1.2 m belowground, and lower fan groundwater ranging from 1.2 to 1.9 m belowground. Each of these source areas ranged only between 5 and 20 m laterally from the stream (Table 2). One exception occurred during the spring hydrologic season, with groundwater contributions from the deepest groundwater well at site A3 (A3S4), which was installed 3.8 m belowground and 59.6 m laterally from the stream. At each site, the relative contributions from the upstream end-member decreased from spring to summer and fall hydrologic seasons. This was particularly pronounced at the upper catchment sites A2 and A3. Upstream contributions to streamflow declined 17.7% from spring to fall at site A2, and 33.3% at site A3. At site AB3, upstream contributions to streamflow only declined slightly between hydrologic season but shifted in which upstream reach was the major contributor (51.3% contributions from upstream A in spring to 48.8% contributions from upstream B in the fall). This switch between contributions from upstream A in the spring and summer to upstream B during fall was unexpected given the intermittency of surface flow in reach B. However, this result aligns with our geochemical characterization along the longitudinal stream profile, with site AB3 becoming more chemically similar to reach B for most solutes during fall months (Fig. 6).

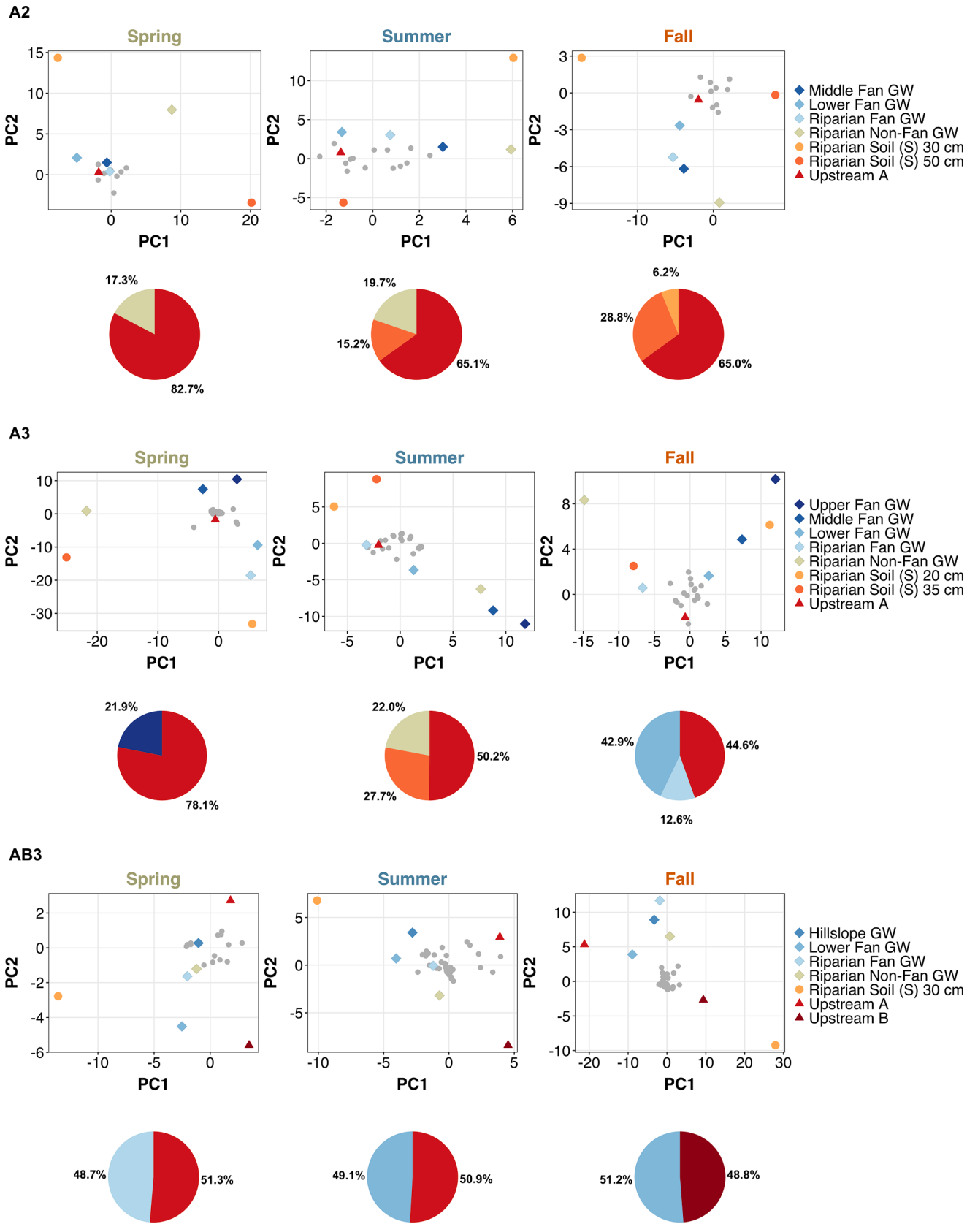

Fig. 7. Two-dimensional principal component analysis (PCA) results and their relative contributions for each site (A2, A3 and AB3) and across each hydrologic season calculated in end-member mixing analysis (EMMA). Stream samples are symbolized with grey circles. Average relative proportion of contributions for each mixing scenario are displayed in pie diagrams beneath each end-member mixing scenario projected into principal component space. Rainfall, snow, and zero-tension soil lysimeters clustered too distantly from the stream sample clusters to visualize all potential end-members.

Table 5
R^2 values and slope parameters (in parentheses) of least-squares linear regressions between observed stream solute concentrations and stream solute concentrations back-calculated from mixing model results. Linear regressions were calculated with the observed concentration (y) as a function of the back-calculated value (x).

Hydrologic Season	Site	End-members	Tracer	R^2	Slope
Spring	A2	Riparian Non-Fan GW	K	0.66	−0.84
		Upstream A	Mg	0.94	1.78
			F	0.59	1.09
			SO_4	0.99	0.52
	A3	Upper Fan GW	K	0.49	1.12
		Upstream A	Mg	0.76	0.44
			F	0.60	0.67
			SO_4	0.93	1.10
	AB3	Riparian Fan GW	Mg	0.72	1.41
		Upstream A	Cl	0.51	0.21
			SO_4	0.89	3.02
Summer	A2	Riparian Non-Fan GW	K	0.10	−3.08
		Riparian Soil (S) 50 cm	Mg	0.73	1.04
		Upstream A	F	0.43	0.63
			SO_4	0.74	−0.41
	A3	Riparian Non-Fan GW	K	0.89	1.31
		Riparian Soil (S) 35 cm	Mg	0.51	0.36
		Upstream A	F	0.31	1.06
			SO_4	0.92	1.82
	AB3	Lower Fan GW	Mg	0.26	1.04
		Upstream A	Cl	0.99	1.35
			SO_4	0.93	2.14
Fall	A2	Riparian Soil (S) 30 cm	K	0.10	0.11
		Riparian Soil (S) 50 cm	Mg	0.86	5.12
		Upstream A	F	0.10	−0.13
			SO_4	0.94	1.20
	A3	Lower Fan GW	K	0.51	0.99
		Riparian Fan GW	Mg	0.19	0.94
		Upstream A	F	0.41	0.66
			SO_4	0.50	1.94
	AB3	Upstream A	Mg	0.97	2.27
		Upstream B	Cl	0.78	1.13
			SO_4	0.87	1.48

Conceptually, our results indicate that the greatest contribution to longitudinal streamflow is generated during spring snowmelt at the headwaters of the catchment, as represented by the upstream chemical signature in our EMMA results (Fig. 7). We propose a conceptual model of the observed seasonal changes in dominant streamflow contributions within this montane headwater catchment (Fig. 8). Our hydrometric characterization of groundwater and soil moisture levels indicated that as the system shifts from the start of the spring hydrologic season (early season) to the end of the fall hydrologic season (late season), catchment wetness and groundwater levels decline. From early to late season, upstream source areas become less important to sustaining streamflow of downstream reaches and lateral contributions from groundwater and soil water adjacent to the stream become more important to sustaining streamflow (Fig. 8). These findings are significant given the small size of Hotel Stream – the maximum specific discharge we observed at the three study sites was 0.03 mm hr^{-1} (measured during the spring hydrologic season). In the case of site AB3, an ~50% relative contribution from laterally connected groundwater would provide a substantial source of water to the stream, particularly as the overall moisture content of the catchment decreases into the fall hydrologic season. Therefore, connection to local groundwater source areas at the reach level become increasingly important to maintaining streamflow through time.

4.2. Lateral upslope accumulation areas are important source areas to the stream, but to what extent?

We anticipated and our results supported that landscape units with high lateral UAA would be a first-order control to stream connectivity as found in Jencso et al. (2009) and Bergstrom et al. (2016). These findings are consistent with the foundational hillslope hydrology studies that found a connection between UAA (or contributing area), and the accumulation of subsurface flow (e.g., Anderson & Burt, 1978; Beven & Kirkby, 1979; Dunne & Black, 1970; Harr, 1977; Hewlett & Hibbert, 1967). During the spring hydrologic season in particular, we expected the highest proportion of the catchment to be hydrologically active as a result of snowmelt saturating soils and increasing groundwater levels (Bergstrom et al., 2016; Bukoski et al., 2021; Harrison et al., 2021; Jencso et al., 2009; McNamara et al., 2005; Nippgen et al., 2015). By extension, we expected hydrologic connectivity between the most laterally distant (upland) portions of the alluvial/ colluvial fans and the stream. During snowmelt in the Tenderfoot Creek Experimental Forest in central Montana, USA, for example, Bergstrom et al. (2016) found a strong relationship between lateral contributing area and gross gains in streamflow. However, our geochemical characterizations of groundwater and soil water indicate that upland fan source areas were not a major contributor to stream chemistry. The lack of connection between the furthest upland portions of the fan sites and the stream is consistent with the findings of Gregory et al. (2022); within Hotel Gulch, comparisons of stream and soil molar ratios of major cations and anions suggested a lack of connection between soils from non-riparian

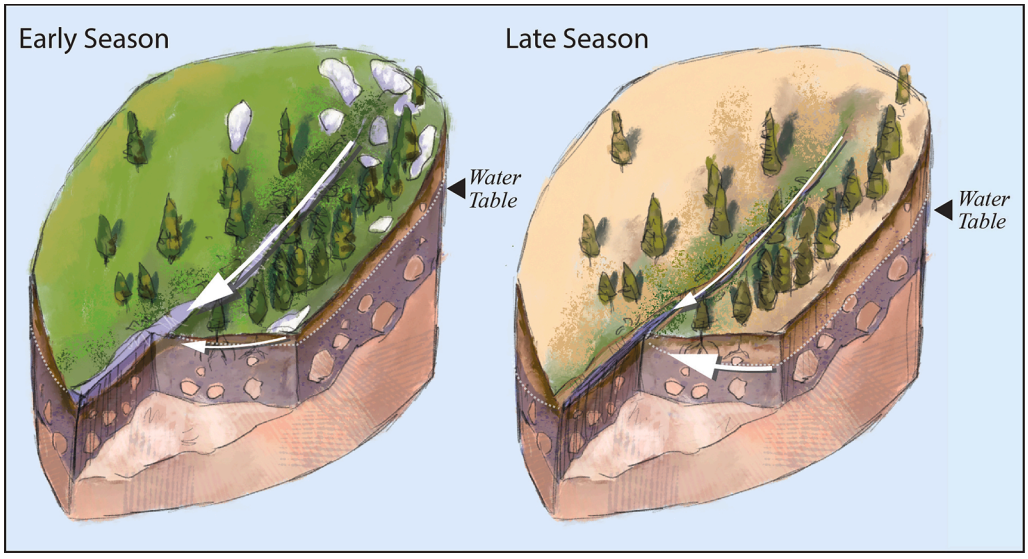

Fig. 8. Conceptual diagram showing how dominant source areas to streamflow shift seasonally from longitudinal to lateral contributions in Hotel Gulch. The sizes of the arrows are representative of relative proportions of longitudinal and lateral contributions to streamflow. During the early season when groundwater levels and overall catchment moisture are highest, streamflow is largely sustained by upstream, or longitudinal, contributions. During the late season when groundwater levels and overall catchment moisture have declined, streamflow is largely sustained by adjacent soil and groundwater, or lateral, contributions. Illustration credit: Eric Parrish.

landscape units and the stream. Our findings combined with Gregory et al. (2022) may also be indicative of contributions from deeper flow paths as in Hornberger et al. (1998). Due to the relatively shallow depths of our groundwater wells, we likely were only able to capture the activation of such deeper flow paths at our deepest groundwater well (A3S4) during spring snowmelt (Fig. 7). Further characterizing these deep groundwater flowpaths would allow for a more insightful analysis of subsurface contributions to streamflow but is beyond the scope of this study.

At the upper fan sites A2 and A3, the deepest and furthest source area appeared to be hydrologically connected to the stream during the spring (Fig. 7), with a shift to shallow riparian contributions as the catchment dried down into the summer (Fig. 4, Supplementary Fig. 2). Previous studies have found similar patterns in connectivity: as overall catchment moisture and streamflow declines, contributing area becomes a less important control of streamflow, and connectivity is limited to near stream source areas (Bergstrom et al., 2016; Kiewiet et al., 2020; Nippgen et al., 2015; Payn et al., 2012; Smith et al, 2013). Smith et al. (2013) found that only approximately 5% of the stream network was hydrologically connected to the catchment through shallow subsurface flow during periods of low-flow. Similarly, Nippgen et al. (2015) found that simulated connected area expanded from areas parallel and close to the stream during low-flow conditions to upland hillslopes during high-flow conditions. While our results indicate a lack of prolonged connectivity between the most upland source areas and the stream, our EMMA results indicate substantial and sustained lateral stream contributions up to approximately 20 m.

4.3. Implications for montane headwater systems

Understanding the sources and timing of water delivery to streams is a fundamental topic in hydrologic research. While topographic features and landscape processes are unique to each study – including the alluvial/ colluvial fans in this work – our findings provide valuable insight into the spatiotemporal shifts of dominant source areas to streamflow. Understanding the dynamic nature of active and connected source areas within a catchment is critical to understanding shifts in downstream water quantity and quality, with impacts for water resource management, as well as ecosystem services and ecosystem health (Acuña et al., 2014; Buttle et al., 2012; Stubbington et al., 2017). For example, Pacific et al. (2010) found that the transport of dissolved organic carbon (DOC) to the stream network was highly dependent on the connectivity of specific source areas with high DOC concentrations. In addition, disturbances like anthropogenic land use change and wildfire have been shown to impact downstream water quality (e.g., Bolstad and Swank, 1997; Clinton & Vose, 2006; Gardner et al., 2011; Murphy et al., 2018). The Upper South Platte River Basin where our study was conducted, is both a highly fire-prone and erosive landscape (Graham, 2003). Prior to 2020, the Upper South Platte was the site of the largest fire in Colorado history (Hayman Fire now ranked 4th largest). Wildfire can also alter runoff processes, causing shifts in subsurface flow, and impacting the quantity and quality of water delivered from uplands to streams (Ebel et al., 2012; Moody and Ebel, 2014). Within the context of this study, if climate variability or disturbance were to disrupt the subsurface flow between laterally connected groundwater, for example, the streamflow could decrease up to 50%, negatively impacting downstream ecosystem health.

4.4. Limitations of the study

We used EMMA to elucidate patterns in source area stream contributions from a multiyear stream chemistry dataset and across hydrological seasons. In doing so, we were able to examine shifts in source area contributions under a variety of spatiotemporal conditions. However, as with all studies utilizing EMMA, our results are limited by our degree of success in accurately characterizing the geochemistry of all potential end-members, and the conservative behavior of the tracers used (Burns et al, 2001). Tracers used for each EMMA model were screened for non-conservative behavior, and bivariate solutes plots revealed linear relationships for reach A and reach AB tracers ($r^2 > 0.5$, p-value < 0.01). Additionally, each tracer selected was approximately normally distributed (Shapiro-wilk p-value > 0.05), improving the robustness of each mixing scenario. However, selected tracers at certain sites and during certain hydrologic seasons were less successful in reproducing observed fluctuations in stream chemistry (poor mixing model fitness) (Table 5). We attribute poor mixing model fitness to the fact that the same tracer selection procedure was carried out and applied to all hydrologic seasons, and to both reach A sites. A single tracer selection was based on the whole stream chemistry data set for sites A2 and A3. However, using a single tracer selection was necessary for comparisons between end-members and relative contributions among mixing scenarios along each stream reach. We chose to evaluate reach AB separately from reach A due to inputs from non-perennial stream B (Fig. 2). As a result, mixing model fitness was generally improved at site AB3 compared to A2 and A3. Because the same tracers were applied across all hydrologic seasons, certain tracers still did not perform as well during some seasons compared to others (e.g., Mg during summer at site AB3). This was observed across all sites and hydrologic seasons. We attribute this to the selected tracers reflecting connectivity to a specific source area of the catchment (e.g., Pacific et al., 2010) through different hydrologic seasons, rather than to catchment-wide connectivity across all seasons.

5. Conclusions

Streamflow sources across hydrologic seasons were characterized in a 2.65 km^2 semi-arid montane headwater catchment. We used a combined approach of hydrometric monitoring, geochemical characterization and end-member mixing analysis to assess hydrologic connectivity of the catchment with high upslope accumulation area (UAA). The areas with highest UAA corresponded to alluvial/ colluvial fans wherein we focused instrumentation and water sample collection to address lateral, longitudinal, and vertical connectivity between the landscape and the stream. We used observed rainfall trends to determine hydrologic seasons spanning from May through October, reflecting different conditions with respect to stream discharge, soil moisture, and groundwater levels. Using end-member mixing analysis, we found that source areas to streamflow shifted in space in time, with contributions from upstream sites becoming less important than lateral contributions between spring, summer, and fall hydrologic seasons. Our results indicate dynamic shifts in hydrologic connectivity in space and in time, which are increasingly important to land and water resource management within the western United States.

CRediT authorship contribution statement

Sidney A. Bush: Conceptualization, Methodology, Software, Formal analysis, Investigation, Data curation, Visualization, Writing – original draft. **Andrew L. Birch:** Conceptualization, Methodology, Software, Formal analysis, Writing – review & editing. **Sara R. Warix:** Investigation, Writing – review & editing. **Pamela L. Sullivan:** Conceptualization, Validation, Writing – review & editing, Project administration, Funding acquisition. **Michael N. Gooseff:** Conceptualization, Resources, Writing – review & editing. **Diane M. McKnight:** Conceptualization, Writing – review & editing. **Holly R. Barnard:** Conceptualization, Methodology, Validation, Resources, Writing – review & editing, Supervision, Project administration, Funding acquisition.

Declaration of Competing Interest

The authors declare that they have no known competing financial

interests or personal relationships that could have appeared to influence the work reported in this paper.

Data availability

The raw data used for analysis supporting the conclusions herein can be accessed through the CUAHSI HydroShare data repository: http://www.hydroshare.org/resource/f4edbcd9aec9490da06ff49297ad3932.

Acknowledgements

Funding for this research was provided by NSF Award numbers 2012669, 2012796, and 2116687. We would like to acknowledge the site manager, Steve Alton, and the scientist in charge, Paula Fornwalt at the Manitou Experimental Forest for their extensive collaboration and coordination for this research. We thank Nicole Hornslein, Reece Gregory, Mykael Pineda, Matthew Schiff, and Austin Gore for field and lab assistance. We thank Isaac Bukoski, Stephanie Jarvis, Meggi Vernai, Lacey Allor, and Reed Kuykendall for field assistance. We also thank Keira Johnson for collaboration with SNODAS estimates. The conceptual diagram shown in Fig. 8 was illustrated by Eric Parrish. Lastly, we thank the two anonymous reviewers for their helpful comments and constructive suggestions. The raw data used for analysis supporting the conclusions herein can be accessed through the CUAHSI HydroShare data repository: http://www.hydroshare.org/resource/f4edbcd9aec9490da06ff49297ad3932.

Appendix A. Supplementary data

Supplementary data to this article can be found online at https://doi.org/10.1016/j.jhydrol.2023.129134.

References

Acuña, V., Datry, T., Marshall, J., Barceló, D., Dahm, C.N., Ginebreda, A., Mcgregor, G., Sabater, S., Tockner, K., Palmer, M.A., 2014. Why should we care about temporary waterways? Science 343, 1080–1081. https://doi.org/10.1126/science.1246666.

Adams, J. (2021, June 29). *Where does your water come from?* Retrieved from https://www.denverwater.org/tap/where-does-your-water-come.

Anderson, M.G., Burt, T.P., 1978. The role of topography in controlling throughflow generation. Earth Surface Process. 3 (4), 331–344.

Bergstrom, A., Jencso, K., McGlynn, B., 2016. Spatiotemporal processes that contribute to hydrologic exchange between hillslopes, valley bottoms, and streams. Water Resour. Res. 52, 4628–4645. https://doi.org/10.1002/2015WR017972.

Berkelhammer, M., Noone, D.C., Wong, T.E., Burns, S.P., Knowles, J.F., Kaushik, A., Blanken, P.D., Williams, M.W., 2016. Convergent approaches to determine an ecosystem's transpiration fraction. Global Biogeochem. Cycles 30, 933–951. https://doi.org/10.1002/2016GB005392.

Beven, K., Kirkby, M., 1979. A physically based, variable contributing area model of basin hydrology. Hydrol. Sci. Bull. 24 (1), 43–69.

Birch, A.L., Stallard, R.F., Bush, S.A., Barnard, H.R., 2021. The influence of land cover and storm magnitude on hydrologic flowpath activation and runoff generation in steep tropical catchments of central Panama. J. Hydrol. 596, 126138 https://doi.org/10.1016/j.jhydrol.2021.126138.

Blume, T., van Meerveld, H.J.I., 2015. From hillslope to stream: methods to investigate subsurface connectivity. WIREs Water 2, 177–198. https://doi.org/10.1002/wat2.1071.

Bolstad, P.V., Swank, W.T., 1997. Cumulative impacts of landuse on water quality in a southern appalachian watershed 1. JAWRA J. Am. Water Resour. Assoc. 33 (3), 519–533.

Bracken, L.J., Croke, J., 2007. The concept of hydrological connectivity and its contribution to understanding runoff-dominated geomorphic systems. Hydrol. Process. 21, 1749–1763. https://doi.org/10.1002/hyp.6313.

Bukoski, I.S., Murphy, S.F., Birch, A.L., Barnard, H.R., 2021. Summer runoff generation in foothill catchments of the Colorado Front Range. J. Hydrol. 595, 125672.

Burns, D.A., McDonnell, J.J., Hooper, R.P., Peters, N.E., Freer, J.E., Kendall, C., Beven, K., 2001. Quantifying contributions to storm runoff through end-member mixing analysis and hydrologic measurements at the Panola Mountain Research Watershed (Georgia, USA). Hydrol. Process. 15 (10), 1903–1924.

Buttle, J.M., Boon, S., Peters, D.L., Spence, C., (Ilja) van Meerveld, H.J., Whitfield, P.H., 2012. An overview of temporary stream hydrology in Canada. Can. Water Resour. J. / Rev Can. des ressources hydriques 37 (4), 279–310.

Cattell, R.B., 1966. The scree test for the number of factors. Multivar. Behav. Res. 1 (2), 245–276.

Christophersen, N., Hooper, R.P., 1992. Multivariate analysis of stream water chemical data' the use of principal components analysis for the end-member mixing problem. Water Resour. Res. 28, 99–107. https://doi.org/10.1029/91WR02518.

Clinton, B.D., Vose, J.M., 2006. Variation in stream water quality in an urban headwater stream in the southern Appalachians. Water Air Soil Pollut. 169 (1), 331–353.

Covino, T., 2017. Hydrologic connectivity as a framework for understanding biogeochemical flux through watersheds and along fluvial networks. Geomorphology 277, 133–144. https://doi.org/10.1016/j.geomorph.2016.09.030.

Cowie, R.M., Knowles, J.F., Dailey, K.R., Williams, M.W., Mills, T.J., Molotch, N.P., 2017. Sources of streamflow along a headwater catchment elevational gradient. J. Hydrol. 549, 163–178. https://doi.org/10.1016/j.jhydrol.2017.03.044.

D'Odorico, P., Rigon, R., 2003. Hillslope and channel contributions to the hydrologic response. Water Resour. Res. 39 (5), 1113. https://doi.org/10.1029/2002WR001708.

Dunne, T., Black, R.D., 1970. Partial area contributions to storm runoff in a small New England watershed. Water Resour. Res. 6 (5), 1296–1311. https://doi.org/10.1029/WR006i005p01296.

Ebel, B.A., Moody, J.A., Martin, D.A., 2012. Hydrologic conditions controlling runoff generation immediately after wildfire. Water Resour. Res. 48 (3).

Eng, K., Wolock, D.M., Dettinger, M.D., 2016. Sensitivity of intermittent streams to climate variations in the USA. River Res. Appli. 32, 885–895. https://doi.org/10.1002/rra.2939.

Frank, John M.; Fornwalt, Paula J.; Asherin, Lance A.; Alton, Steven K. 2021. Manitou Experimental Forest hourly meteorology data. 3rd ed., Fort Collins, CO: Forest Service Research Data Archive. https://doi.org/10.2737/RDS-2011-0001-3.

Fritze, H., Stewart, I.T., Pebesma, E., 2011. Shifts in Western North American snowmelt runoff regimes for the recent warm decades. J. Hydrometeor. 12, 989–1006. https://doi.org/10.1175/2011JHM1360.1.

Gardner, K.K., McGlynn, B.L., Marshall, L.A., 2011. Quantifying watershed sensitivity to spatially variable N loading and the relative importance of watershed N retention mechanisms. Water Resour. Res. 47, W08524. https://doi.org/10.1029/2010WR009738.

Godsey, S.E., Kirchner, J.W., 2014. Dynamic, discontinuous stream networks: hydrologically driven variations in active drainage density, flowing channels and stream order. Hydrol. Process. 28, 5791–5803. https://doi.org/10.1002/hyp.10310.

Graham, Russell T. 2003. Hayman Fire case study: Summary [RMRS-GTR-114]. In: Graham, Russell T., Technical Editor. Hayman Fire Case Study. Gen. Tech. Rep. RMRS-GTR-114. Ogden, UT: U.S. Department of Agriculture, Forest Service, Rocky Mountain Research Station. p. 1-32.

Gregory, R.B., Bush, S.A., Sullivan, P.L., Barnard, H.R., 2022. Examining spatial variation in soil solutes and flowpaths in a semi-arid, montane catchment. Front. Water 4, 1003968. https://doi.org/10.3389/frwa.2022.1003968.

Hammond, J.C., Saavedra, F.A., Kampf, S.K., 2018. How does snow persistence relate to annual streamflow in mountain watersheds of the western US with wet maritime and dry continental climates? Water Resour. Res. 54 (4), 2605–2623.

Harr, R.D., 1977. Water flux in soil and subsoil on a steep forested slope. J. Hydrol. 33 (1-2), 37–58.

Harrison, H.N., Hammond, J.C., Kampf, S., Kiewiet, L., 2021. On the hydrological difference between catchments above and below the intermittent-persistent snow transition. Hydrol. Process. 35 (11), e14411.

Hewlett, J.D., Hibbert, A.R., 1967. Factors affecting the response of small watersheds to precipitation in humid areas. In: Sopper, W.E., Lull, H.W. (Eds.), International Symposium on Forest Hydrology. Pergamon, Oxford, UK, pp. 275–290.

Hinckley, E.L.S., Ebel, B.A., Barnes, R.T., Anderson, R.S., Williams, M.W., Anderson, S.P., 2014. Aspect control of water movements on hillslopes near the rain-snow transition of the Colorado front range. Hydrol. Process. 28 (1), 74–85.

Hooper, R.P., Christophersen, N., Peters, N.E., 1990. Modelling streamwater chemistry as a mixture of soilwater end-members – An application to the Panola Mountain catchment, Georgia, U.S.A. J. Hydrol. 116, 321–343. https://doi.org/10.1016/0022-1694(90)90131-G.

Hooper, R.P., Shoemaker, C.A., 1986. A comparison of chemical and iootopic hydrograph separation. Water Resour. Res. 22, 1444–1454. https://doi.org/10.1029/WR022i010p01444.

Hopp, L., McDonnell, J.J., 2009. Connectivity at the hillslope scale: Identifying interactions between storm size, bedrock permeability, slope angle and soil depth. J. Hydrol. 376, 378–391. https://doi.org/10.1016/j.jhydrol.2009.07.047.

Hornberger, G.M., Raffensperger, J.P., Wiberg, P.L., Eshleman, K.N., 1998. Elements of Physical Hydrology. Johns Hopkins University Press, Baltimore, Md.

Hu, J., Moore, D.J.P., Burns, S.P., Monson, R.K., 2010. Longer growing seasons lead to less carbon sequestration by a subalpine forest. Glob. Chang. Biol. 16, 771–783. https://doi.org/10.1111/j.1365-2486.2009.01967.x.

Hunsaker, C.T., Whitaker, T.W., Bales, R.C., 2012. Snowmelt runoff and water yield along elevation and temperature gradients in California's Southern Sierra Nevada 1. JAWRA J. Am. Water Resour. Assoc. 48 (4), 667–678.

Jacobs, J., 2011. The sustainability of water resources in the Colorado River basin. Bridge 41 (4), 6–12.

Jencso, K.G., McGlynn, B.L., 2011. Hierarchical controls on runoff generation: topographically driven hydrologic connectivity, geology, and vegetation. Water Resour. Res. 47, W11527. https://doi.org/10.1029/2011WR010666.

Jencso, K.G., McGlynn, B.L., Gooseff, M.N., Wondzell, S.M., Bencala, K.E., Marshall, L.A., 2009. Hydrologic connectivity between landscapes and streams: Transferring reach- and plot-scale understanding to the catchment scale. Water Resour. Res. 45, W04428.

Kampf, S.K., Lefsky, M.A., 2016. Transition of dominant peak flow source from snowmelt to rainfall along the Colorado Front Range: historical patterns, trends, and lessons

from the 2013 colorado front range floods. Water Resour. Res. 52, 407–422. https://doi.org/10.1002/2015WR017784.
Kampf, S., Markus, J., Heath, J., Moore, C., 2015. Snowmelt runoff and soil moisture dynamics on steep subalpine hillslopes. Hydrol. Processes 29 (5), 712–723. https://doi.org/10.1002/hyp.10179.
Kiewiet, L., van Meerveld, I., Stähli, M., Seibert, J., 2020. Do stream water solute concentrations reflect when connectivity occurs in a small, pre-Alpine headwater catchment? Hydrol. Earth Syst. Sci. 24, 3381–3398. https://doi.org/10.5194/hess-24-3381-2020.
Klos, P.Z., Link, T.E., Abatzoglou, J.T., 2014. Extent of the rain-snow transition zone in the western U.S. under historic and projected climate. Geophys. Res. Lett. 41, 4560–4568. https://doi.org/10.1002/2014GL060500.
Lindsay, J.B., 2016. Whitebox GAT: A case study in geomorphometric analysis. Comput. Geosci. 95, 75–84. https://doi.org/10.1016/j.cageo.2016.07.003.
Linkhart, B.D., 2001. Life History Characteristics and Habitat Quality of Flammulated Owls (Otus flammeolus) in Colorado. University of Colorado, Boulder, CO U.S.A. Ph. D. dissertation,.
Liu, F., Hunsaker, C., Bales, R.C., 2013. Controls of streamflow generation in small catchments across the snow–rain transition in the Southern Sierra Nevada, California. *Hydrol. Process.* 27 (14), 1959–1972.
Liu, F.J., Williams, M.W., Caine, N., 2004. Source waters and flow paths in an alpine catchment, Colorado Front Range, United States. Water Resour. Res. 40, W09401. https://doi.org/10.1029/2004WR003076.
Marchand, P., Johnson, S., Drossman, H., 2006. Long-term effects of mechanical fuel treatments, Manitou Experimental Forest, Colorado: First-year results. Research Joint Venture Agreement 04-JV-11221616-298. Catamount Center for Geography of the Southern Rockies, Woodland Park, CO, p. 29.
McGlynn, B.L., McDonnell, J.J., 2003. Quantifying the relative contributions of riparian and hillslope zones to catchment runoff. Water Resour. Res. 39 (11), 1310. https://doi.org/10.1029/2003WR002091.
McNamara, J.P., Chandler, D., Seyfried, M., Achet, S., 2005. Soil moisture states, lateral flow, and streamflow generation in a semi-arid, snowmelt-driven catchment. Hydrol. Processes: Int. J. 19 (20), 4023–4038.
Moody, J.A., Ebel, B.A., 2014. Infiltration and runoff generation processes in fire-affected soils. Hydrol. Process. 28 (9), 3432–3453.
Moore, C., Kampf, S., Stone, B., Richer, E., 2015. A GIS-based method for defining snow zones: application to the western United States. Geocarto Int. 30 (1), 62–81.
Moore, R.D. 2004. Introduction to salt dilution gauging for streamflow measurement: Part 1. Streamline Watershed Management Bulletin 7(4):20–23.
Murphy, S.F., McCleskey, R.B., Martin, D.A., Writer, J.H., Ebel, B.A., 2018. Fire, flood, and drought: Extreme climate events alter flow paths and stream chemistry. J. Geophys. Res. Biogeo. 123 (8), 2513–2526.
Nadeau, T.-L., Rains, M.C., 2007. Hydrological connectivity between headwater streams and downstream waters: how science can inform policy. JAWRA *J. Am. Water Resour. Assoc.* 43, 118–133. https://doi.org/10.1111/j.1752-1688.2007.00010.x.
National Operational Hydrologic Remote Sensing Center. 2004. Snow Data Assimilation System (SNODAS) Data Products at NSIDC, Version 1. Boulder, Colorado USA. NSIDC: National Snow and Ice Data Center. https://doi.org/10.7265/N5TB14TC.
Nippgen, F., McGlynn, B.L., Marshall, L.A., Emanuel, R.E., 2011. Landscape structure and climate influences on hydrologic response. Water Resour. Res. 47 (12).
Nippgen, F., Mcglynn, B.L., Emanuel, R.E., 2015. The spatial and temporal evolution of contributing areas. Water Resour. Res. 51, 4550–4573. https://doi.org/10.1002/2014WR016719.
Ortega, J., Turnipseed, A., Guenther, A.B., Karl, T.G., Day, D.A., Gochis, D., Huffman, J. A., Prenni, A.J., Levin, E.J.T., Krei-denweis, S.M., DeMott, P.J., Tobo, Y., Patton, E. G., Hodzic, A., Cui, Y.Y., Harley, P.C., Hornbrook, R.S., Apel, E.C., Monson, R.K., Eller, A.S.D., Greenberg, J.P., Barth, M.C., Campuzano-Jost, P., Palm, B.B., Jimenez, J.L., Aiken, A.C., Dubey, M.K., Geron, C., Offenberg, J., Ryan, M.G., Fornwalt, P.J., Pryor, S.C., Keutsch, F.N., DiGangi, J.P., Chan, A.W.H., Goldstein, A. H., Wolfe, G.M., Kim, S., Kaser, L., Schnitzhofer, R., Hansel, A., Cantrell, C.A., Mauldin, R.L., Smith, J.N., 2014. Overview of the Manitou Experimental Forest Observatory: site description and selected science results from 2008 to 2013. Atmos. Chem. Phys. 14, 6345–6367. https://doi.org/10.5194/acp-14-6345-2014.
Pacific, V.J., Jencso, K.G., McGlynn, B.L., 2010. Variable flushing mechanisms and landscape structure control stream DOC export during snowmelt in a set of nested catchments. Biogeochemistry 99 (1), 193–211.
Payn, R.A., Gooseff, M.N., McGlynn, B.L., Bencala, K.E., Wondzell, S.M., 2012. Exploring changes in the spatial distribution of stream baseflow generation during a seasonal recession. Water Resour. Res. 48, W04519. https://doi.org/10.1029/2011WR011552.
Phillips, R.W., Spence, C., Pomeroy, J.W., 2011. Connectivity and runoff dynamics in heterogeneous basins. Hydrol. Process. 25 (19), 3061–3075. https://doi.org/10.1002/hyp.8123.
Retzer, John L. 1949. Soils and physical conditions of Manitou Experimental Forest. 1949. Fort Collins, CO: U.S. Department of Agriculture, Forest Service, Rocky Mountain Forest and Range Experiment Station. 37 p.
Rossi, M.W., Anderson, S.P., Anderson, R.S. and Tucker, G.E. 2022. Bedrock exposure, canopy density, and runoff generation in the Rampart Range, CO 2018. National Center for Airborne Laser Mapping (NCALM). Distributed by OpenTopography. https://doi.org/10.5069/G9CV4FXZ.
Reges, H.W., Doesken, N., Turner, J., Newman, N., Bergantino, A., Schwalbe, Z., 2016. COCORAHS: The evolution and accomplishments of a volunteer rain gauge network. Bull. Amer. Meteor. Soc. 97, 1831–1846. https://doi.org/10.1175/BAMS-D-14-00213.1.
Seibert, J., McGlynn, B.L., 2007. A new triangular multiple flow direction algorithm for computing upslope areas from gridded digital elevation models. Water Resour. Res. 43, W04501. https://doi.org/10.1029/2006WR005128.
Sklash, M.G., Farvolden, R.N., 1979. The role of groundwater in storm runoff. J. Hydrol. 43, 45–65. https://doi.org/10.1016/0022-1694(79)90164-1.
Smith, T., Marshall, L., McGlynn, B., Jencso, K., 2013. Using field data to inform and evaluate a new model of catchment hydrologic connectivity. Water Resour. Res. 49, 6834–6846. https://doi.org/10.1002/wrcr.20546.
Smith, T.J., McNamara, J.P., Flores, A.N., Gribb, M.M., Aishlin, P.S., Benner, S.G., 2011. Small soil storage capacity limits benefit of winter snowpack to upland vegetation. Hydrol. Process. 25 (25), 3858–3865.
Soil Survey Staff, Natural Resources Conservation Service, United States Department of Agriculture (2022) Custom Soil Resource Report for Pike National Forest, Eastern Part, Colorado, Parts of Douglas, El Paso, Jefferson, and Teller Counties.
Soil Survey Staff, Natural Resources Conservation Service, United States Department of Agriculture (2010) U.S. General Soil Map (STATSGO2). Available online. https://data.nal.usda.gov/dataset/united-states-general-soil-map-statsgo2.
Stieglitz, M., Shaman, J., McNamara, J., Engel, V., Shanley, J., Kling, G.W., 2003. An approach to understanding hydrologic connectivity on the hillslope and the implications for nutrient transport. Global Biogeochem. Cycles 17 (4).
Stubbington, R., England, J., Wood, P.J., Sefton, C.E., 2017. Temporary streams in temperate zones: recognizing, monitoring and restoring transitional aquatic-terrestrial ecosystems. Wiley Interdiscip. Rev Water 4. https://doi.org/10.1002/wat2.1223. Article e1223.
Tague, C., Grant, G., Farrell, M., Choate, J., Jefferson, A., 2008. Deep groundwater mediates streamflow response to climate warming in the Oregon Cascades. Clim. Change 86 (1–2), 189–210. https://doi.org/10.1007/s10584-007-9294-8.
Tetzlaff, D., Buttle, J., Carey, S.K., Mcguire, K., Laudon, H., Soulsby, C., 2015. Tracer-based assessment of flow paths, storage and runoff generation in northern catchments: A review. Hydrol. Process. 29 (16), 3475–3490. https://doi.org/10.1002/hyp.10412.
Tromp-van Meerveld, H.J., McDonnell, J.J., 2006. Threshold relations in subsurface stormflow: 1. A 147-storm analysis of the Panola hillslope. Water Resour. Res. 42 https://doi.org/10.1029/2004WR003778. W02410.
Uhlenbrook, S., Roser, S., Tilch, N., 2004. Hydrological process representation at the meso-scale: the potential of a distributed, conceptual catchment model. J. Hydrol. 291, 278–296. https://doi.org/10.1016/j.jhydrol.2003.12.038.
van Meerveld, H.J., Seibert, J., Peters, N.E., 2015. Hillslope-riparian-stream connectivity and flow directions at the Panola Mountain Research Watershed. Hydrol. Process. 29, 3556–3574. https://doi.org/10.1002/hyp.10508.
Viviroli, D., Durr, H.H., Messerli, B., Meybeck, M., Weingartner, R., 2007. Mountains of the world, water towers for humanity: typology, mapping, and global significance. Water Resour. Res. 43 (7), W07447. https://doi.org/10.1029/2006WR005653.
Ward, A.S., Wondzell, S.M., Schmadel, N.M., Herzog, S.P., 2020. Climate change causes river network contraction and disconnection in the HJ Andrews Experimental Forest, Oregon, USA. Front. Water 2, 7.
Whiting, J.A., Godsey, S.E., 2016. Discontinuous headwater stream networks with stable flowheads, Salmon River basin, Idaho. Hydrol. Processes 30 (13), 2305–2316. https://doi.org/10.1002/hyp.10790.
Zimmer, M.A., McGlynn, B.L., 2017. Ephemeral and intermittent runoff generation processes in a low relief, highly weathered catchment. Water Resour. Res. 53, 7055–7077. https://doi.org/10.1002/2016WR019742.
Zimmer, M.A., McGlynn, B.L., 2018. Lateral, vertical, and longitudinal source area connectivity drive runoff and carbon export across watershed scales. Water Resour. Res. 54, 1576–1598. https://doi.org/10.1002/2017WR021718.